

Untangling the trees: Revision of the *Calumma nasutum* complex (Squamata: Chamaeleonidae)

DAVID PRÖTZEL^{1,*} MARK D. SCHERZ^{1,2}, FANOMEZANA M. RATSOAVINA³, MIGUEL VENCES² & FRANK GLAW¹

¹ Zoologische Staatssammlung München (ZSM – SNSB), Münchhausenstr. 21, 81247 München, Germany — ² Zoological Institute, Braunschweig University of Technology, Mendelssohnstr. 4, 38106 Braunschweig, Germany — ³ Mention Zoologie et Biodiversité Animale, Faculté des Sciences, Université d'Antananarivo, BP 906, Antananarivo, 101 Madagascar — * Corresponding author, e-mail: david.proetzel@mail.de

Submitted March 4, 2019.

Accepted October 10, 2019.

Published online at www.senckenberg.de/vertebrate-zoology on February 4, 2020.

Published in print Q1/2020.

Editor in charge: Uwe Fritz

Abstract

Based on a large number of specimens and genetic samples, we revise the chameleons of the phenetic *Calumma nasutum* species group using an integrative taxonomic approach including external and hemipenial morphology, osteology, and sequences of a mitochondrial (ND2) and a nuclear gene (c-mos). After more than 180 years of taxonomic uncertainty, the eponymous species of the group, *C. nasutum*, is re-described, a lectotype is designated, and the species is assigned to a genetic clade that occurs in eastern (Anosibe An'Ala, Andasibe) and northern Madagascar (Sorata) based on morphology and osteology. The identity of *C. fallax* is also clarified and a lectotype is designated; it occurs at high elevation along the east coast from Andohahela (south) to Mandraka (central east). *Calumma radamanus* is resurrected from synonymy of *C. nasutum*; it lives at low elevations in eastern Madagascar from Tampolo (south) to its type locality Ambatondradama (north). However, up to five deep mitochondrial lineages and high morphological variation are identified within *C. radamanus*, which we consider a species complex still in need of further taxonomic revision. Furthermore, three new species of the *C. nasutum* group are described: *C. emelinae* sp. nov. is distributed in eastern Madagascar (Anosibe An'Ala in the south to Makira in the north), *C. tjiasmantoi* sp. nov. in southeastern Madagascar (from Andohahela in the south to Ranomafana NP in the north), and *C. ratnasariae* sp. nov. is known from the Bealanana District in northern Madagascar. There is only little variation in hemipenial morphology in this group; the cornucula gemina are present in all taxa except the *C. radamanus* complex. Due to this taxonomic revision the protection status of the treated six chameleon species needs to be newly assessed; at least two of the species appear to warrant threatened statuses.

Key words

Calumma nasutum species group; hemipenis morphology; integrative taxonomy; Madagascar; new species; osteology.

Introduction

As one of the first ever chameleon species from Madagascar *Calumma nasutum* was described by Duméril & Bibron in 1836. Since then many new discoveries have followed and 92 chameleon species are currently recognised from the island (GLAW, 2015; PRÖTZEL *et al.*, 2017, 2018a, 2018b; SCHERZ *et al.*, 2018, 2019a; SENTÍS *et al.*, 2018). Among the four Madagascan chameleon genera *Brookesia*, *Calumma*, *Furcifer*, and *Palleon*, especially *Calumma* has contributed to the increase in species numbers, with 13 new species described within the last 15 years (RAXWORTHY & NUSSBAUM, 2006; GEHRING

et al., 2010; GEHRING *et al.*, 2011; PRÖTZEL *et al.*, 2017, 2018a, 2018b). This is a result not only of intensified fieldwork, often in remote areas in Madagascar, but also the use of new methods to detect cryptic diversity. Uncovering cryptic species is crucial for conservation management (BICKFORD *et al.*, 2006); a species thought to be widespread over a great distribution range could in fact be a complex of several species, each of which inhabits only a small area (SCHERZ *et al.* 2019b), such as isolated forest fragments that are highly threatened by deforestation (HARPER *et al.*, 2007), as already shown for *C. juliae*

(PRÖTZEL *et al.*, 2018b). Public attention and touristic development can help to protect the habitats of such micro-endemic chameleon species.

Calumma nasutum was long thought to be a common species distributed across most of Madagascar's humid and sub-humid forests, until a genetic analysis of the phenetic *C. nasutum* species group revealed 33 operational taxonomic units (OTUs) based on a fragment of the mitochondrial ND2 gene (GEHRING *et al.*, 2012). Until that point, the group consisted of seven described species: *C. boettgeri* (Boulenger, 1888), *C. fallax* (Mocquard, 1900), *C. gallus* (Günther, 1877), *C. guibei* (Hillenius, 1959), *C. linotum* (Müller, 1924), *C. nasutum* (Duméril & Bibron, 1836), and *C. vohibola* Gehring, Ratoavina, Vences & Glaw, 2011. The species *C. vatosoa* Andreone, Mattioli, Jesu & Randrianirina, 2001 and *C. peyrierasi* (Brygoo, Blanc & Domergue, 1974) were only later transferred to the *C. nasutum* group (PRÖTZEL *et al.*, 2016), and were accordingly not included in the study of GEHRING *et al.* (2012).

After having clarified the taxonomic status of *C. boettgeri*, *C. guibei*, and *C. linotum* of the *C. boettgeri* species group in previous works (PRÖTZEL *et al.*, 2015, 2017) the identity of *C. nasutum* is still unclear – even ~180 years after its description. The lack of a type locality, conserved morphology within the group, and the absence of genetic data from the type specimens due to their age has prevented the re-definition and re-description of *C. nasutum* so far.

In this work, however, we assign *Calumma nasutum* to a genetic clade based on a large number of specimens using an integrative taxonomic approach including genetic analyses of mitochondrial and nuclear gene sequences, osteology and external and hemipenial morphology. Furthermore, we clarify the identity of *C. fallax*, resurrect the species *C. radamanus* from synonymy with *C. nasutum*, and describe three additional new species.

Material and Methods

Taxon sampling

We studied 150 specimens of the different genetic clades of the *Calumma nasutum* group, excluding species with occipital lobes of the *C. boettgeri* complex, from the collections of the Zoologische Staatssammlung München, Germany (ZSM), the Museum National d'Histoire Naturelle, Paris, France (MNHN), the Senckenberg Naturmuseum, Frankfurt, Germany (SMF), the Museo Regionale di Scienze Naturali, Torino, Italy (MRSN), the Université d'Antananarivo, Département de Biologie Animale (now called 'Mention Zoologie et Biodiversité Animale'), Antananarivo, Madagascar (UADBA), and the Zoologisches Forschungsmuseum Alexander Koenig, Bonn, Germany (ZFMK). Data of all these specimens are provided in suppl. Table 1. The names of the mitochon-

drial clades used throughout this paper follow GEHRING *et al.* (2012) and clades studied here are Clade B, G, H, I, J, and K. Clade A (*C. gallus* complex), clade C (*C. vohibola*), clade D (*C. boettgeri* and *C. linotum*), clade E (*C. gehringi*), and clade F (*C. guibei*) were studied elsewhere or will be studied in future projects.

Specimens of the new taxa described herein were collected in the field by surveying mostly at night. They were fixed in 90% ethanol and transferred to 70% ethanol for long-term storage. Field numbers of preserved specimens and tissue samples refer to the collections of Frank Glaw and Miguel Vences (FGMV, FGZC, MV and ZCMV), Mark D. Scherz (MSZC), David R. Vieites (DRV), Franco Andreone (FN), Angelica Crottini (ACZC), Philip-Sebastian Gehring (PSG), Shea M. Lambert (SML) and Maciej Pabijan (MPFC).

External morphology

The morphological measurements taken from these specimens follow largely ECKHARDT *et al.* (2012), GEHRING *et al.* (2012), and PRÖTZEL *et al.* (2018b). The following characters (see also Table 1) were measured with a digital calliper to the nearest 0.1 mm, counted using a binocular dissecting microscope, evaluated by eye or calculated; the dataset contains 6 continuous, 3 meristic, and 8 qualitative/other characters (excluding the respective ratios): snout-vent length (SVL) from the snout tip (not including the rostral appendage) to the cloaca; tail length (TaL) from the cloaca to the tail tip; total length (TL) as a sum of SVL and TaL; ratio of TaL to SVL (RTaSV); length of the rostral appendage (LRA) from the upper snout tip; ratio of LRA to SVL (RRS); diameter of rostral appendage (DRA), measured dorsoventrally at the widest point; rostral scale integrated in rostral appendage (RSI) presence (+) or absence (-); distinct rostral crest (RC) presence (+) or absence (-); lateral crest (LC), running from the posterior of the eye horizontally, presence (+) or absence (-); temporal crest (TC), running dorsally to the LC, curving toward the midline, presence (+) or absence (-); cranial crest (CC), defined by the lateral ridges of the parietal bone that give an edge to the casque, presence (+); or absence (-); parietal crest (PC) presence (+) or absence (-); casque height (CH), measured from the peak of the casque to the beginning of the dorsal ridge of the torso; dorsal crest (DC) absence (-) or number of dorsal cones visible to the naked eye without the use of a binocular microscope according to ECKHARDT *et al.* (2012); number of supralabial scales (NSL), counted from the first scale next to the rostral to the last scale that borders directly and entirely (with one complete side) to the mouth slit of the upper jaw on the right side (i.e. excluding the small granular scales bordering the rictus); and number of infralabial scales (NIL), analogous to the definition of NSL above, on the right side; upper margin of supralabial scales (UMS) serrated (s) or straight in line (l); axillary pits (AP) presence (+) or absence (-); diameter of largest scale on temporal region (DSCT), measured

Table 1. Diagnostic characters based on morphology (greyed numbers indicate diagnostic characters used in the diagnosis): + present; – absent; (+) usually present; +/- absent or present; f, female; m, male; further abbreviations see Material and Methods; all measurements are in millimetres.

species	clade	sex	sample size	SVL	Tal	TL	RtAsV	LRA	RRS	RSI	RC	LC	TC	CC	PC	CH	DC	NIL	NSL	UMS	AP	DSCT	
<i>C. nasutum</i>	K	m	min-max:	43.1–49.0	43.1–51.8	89.0–100.8	0.92–1.06	2.2–2.6	0.045–0.053	–	+	+	+	(+)	–/+	1.5–2.0	0–12	13–15	12–15	(s)	(+)	0.9–1.6	
			mean:	46.0	46.6	92.6	102%	2.3	5.0%	–	–	–	–	–	–	–	1.7	5.0	13.7	13.7	–	–	1.2
			SD:	2.5	3.7	5.5	6%	0.3	0.4%	–	–	–	–	–	–	–	0.2	6.0	1.2	1.3	–	–	–
<i>C. nasutum</i>	K	f	min-max:	43.0–49.4	37.7–45.7	80.7–95.1	0.88–0.97	1.2–1.5	0.028–0.032	–	+	+	+	(+)	–/+	0.7–1.0	–	13–16	14–15	s	(+)	0.8–1.2	
			mean:	46.4	43.3	89.7	93%	1.4	3.0%	–	–	–	–	–	–	–	0.8	–	14.8	14.3	–	–	1.0
			SD:	2.7	3.8	6.3	4%	0.2	0.2%	–	–	–	–	–	–	–	0.2	–	1.3	0.5	–	–	0.2
<i>C. radamanus</i>	GII	m	min-max:	42.6–49.2	42.3–44.3	84.9–93.5	0.90–0.99	1.4–1.7	0.029–0.036	(+)	+	+	(+)	+	–	0.8–1.5	0–7	12–18	11–15	s	(–)	0.6–0.8	
			mean:	46.1	43.2	89.3	94%	1.5	3.3%	–	–	–	–	–	–	1.1	3.3	13.8	13.5	–	–	0.8	
			SD:	3.0	0.9	4.0	4%	0.2	0.3%	–	–	–	–	–	–	0.4	3.8	2.9	1.9	–	–	–	0.1
<i>C. radamanus</i>	GII	f	min-max:	43.0–49.2	34.0–43.7	77.0–92.9	0.79–0.89	0.2–1.6	0.005–0.034	+/-	(+)	+	+	(+)	–	0.5–0.8	–	13–15	12–14	s	–	0.8–0.9	
			mean:	46.4	39.1	85.5	84%	1.0	2.1%	–	–	–	–	–	–	0.6	–	13.7	12.7	–	–	0.8	
			SD:	4.7	8.1	24.1	5%	0.6	1.4%	–	–	–	–	–	–	0.4	–	2.5	2.0	–	–	0.1	
<i>C. emelinae</i> sp. nov.	B	m	min-max:	46.6–48.7	47–54.5	93.6–103.2	1.01–1.12	2.3–2.9	0.047–0.061	–	+	+	+	+	(+)	0.5–1.1	7–10	14–15	14–16	(l)	–	0.7–0.7	
			mean:	47.7	50.7	98.5	106%	2.5	5.2%	–	–	–	–	–	–	0.8	8.7	14.3	14.7	–	–	0.7	
			SD:	1.1	3.8	4.8	6%	0.3	0.7%	–	–	–	–	–	–	0.3	1.5	0.6	1.2	–	–	–	0.0
<i>C. emelinae</i> sp. nov.	B	f	min-max:	40.1–49.1	38.0–46.7	82.7–95.8	0.82–1.06	1.5–1.8	0.031–0.040	–	+	+	+	+	(–)	0.6–1.6	–	13–15	12–14	(l)	–	0.6–1.0	
			mean:	46.2	42.1	88.3	92%	1.6	3.5%	–	–	–	–	–	–	1.0	–	14.0	13.1	–	–	0.7	
			SD:	3.1	3.2	5.0	8%	0.1	0.3%	–	–	–	–	–	–	0.4	–	1.0	0.9	–	–	0.1	
<i>C. tjiasmantoi</i> sp. nov.	J	m	min-max:	46.8	48.0	94.8	103%	2.0	4.3%	–	+	+	+	+	+	+	1.3	9	16	16	1	–	0.8
			mean:	43.9–46.1	40.2–43.9	84.1–90.0	0.92–0.95	1.1–2.1	0.024–0.046	–	–	–	–	–	–	–	0.7–1.2	–	15–18	15–17	1	(–)	0.6–0.8
			SD:	45.2	42.4	87.5	94%	1.6	3.5%	–	–	–	–	–	–	1.0	–	16.0	15.5	–	–	–	0.7
<i>C. fallax</i>	H	m	min-max:	42.9–50.6	47.3–57.7	90.9–107.3	1.02–1.24	1.8–4.3	0.036–0.085	–	+	+	+	+	–	+	1.6–2.5	6–11	11–15	11–15	1	–	1.1–1.6
			mean:	46.7	52.5	99.2	113%	3.1	6.6%	–	–	–	–	–	–	–	2.0	8.0	12.4	13.1	–	–	1.4
			SD:	3.1	3.9	6.3	7%	0.8	1.7%	–	–	–	–	–	–	–	0.3	2.0	1.6	1.8	–	–	0.2
<i>C. fallax</i>	H	f	min-max:	40.8–50.7	36.5–49.1	77.3–99.8	0.89–1.04	1.7–3.2	0.042–0.076	–	+	+	+	+/-	–	+	0.5–1.3	0–5	10–14	10–14	1	–	1.0–1.8
			mean:	46.5	43.8	90.3	94%	2.7	5.9%	–	–	–	–	–	–	–	0.9	1.0	11.9	12.1	–	–	1.3
			SD:	3.4	3.5	6.5	5%	0.5	1.0%	–	–	–	–	–	–	–	0.3	2.0	1.4	1.2	–	–	0.3
<i>C. ratnasariae</i> sp. nov.	I	m	min-max:	43.9–52.0	53.2–58.7	97.1–110.7	1.12–1.21	1.8–2.3	0.038–0.048	–	+	+	+	+	+	+	1.3–1.5	7–12	11–14	10–13	1	–	1.3–1.5
			mean:	48.0	55.4	103.4	116%	2.0	4.2%	–	–	–	–	–	–	–	1.4	8.7	12.7	11.7	–	–	1.4
			SD:	4.1	2.9	6.9	5%	0.3	0.5%	–	–	–	–	–	–	–	0.1	2.9	1.5	1.5	–	–	0.1
<i>C. ratnasariae</i> sp. nov.	I	f	min-max:	48.7–51.5	46.2–49.5	95.3–101.0	0.94–0.98	2.1–2.2	0.041–0.045	–	+	+	+	+	+	+	0.7–1.0	0–8	12–14	11–12	1	–	1.2–1.6
			mean:	49.8	47.8	97.5	96%	2.1	4.3%	–	–	–	–	–	–	–	0.8	4.7	12.7	11.3	–	–	1.4
			SD:	1.5	1.7	3.0	2%	0.1	0.2%	–	–	–	–	–	–	–	0.2	4.2	1.2	0.6	–	–	0.2

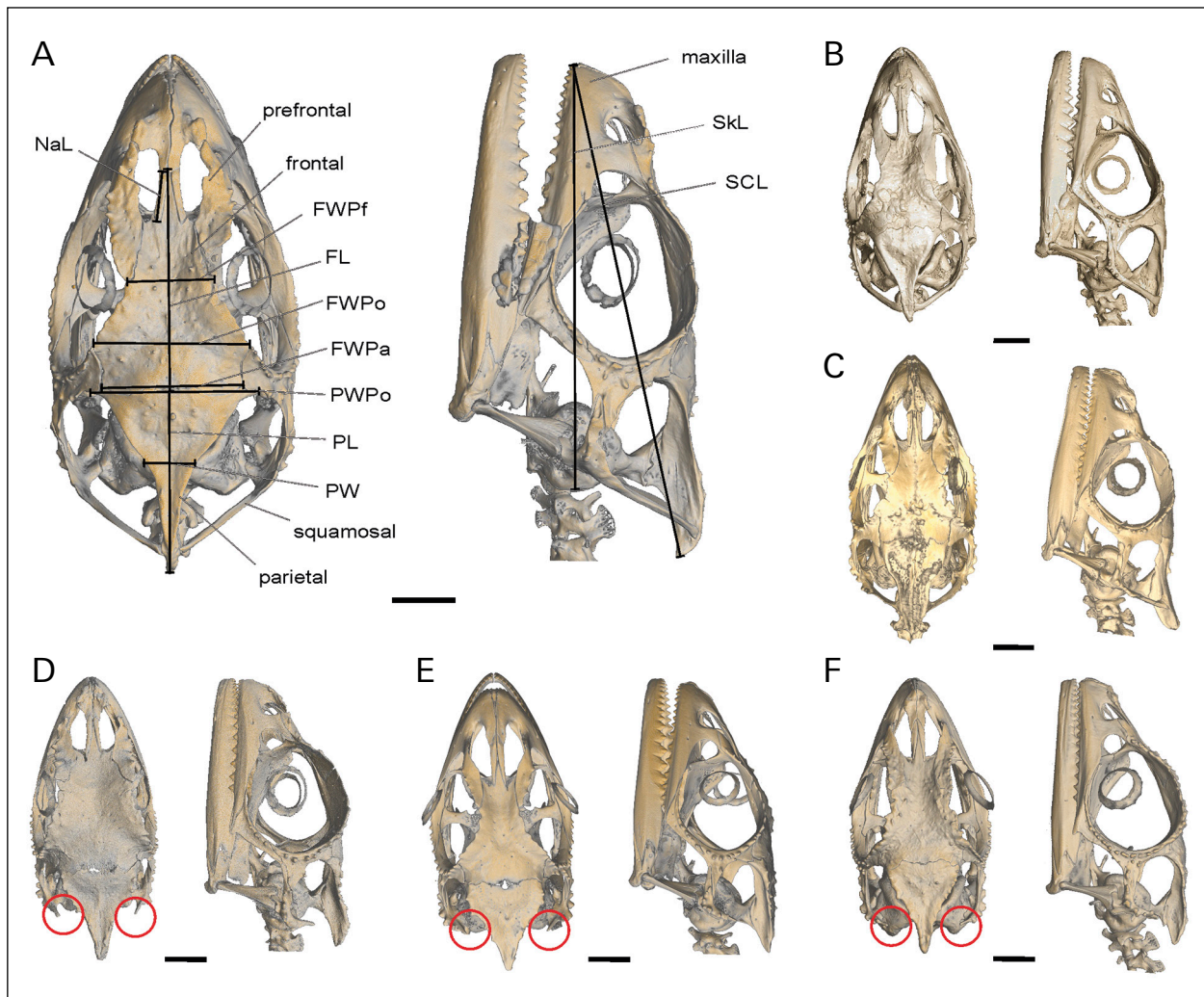


Fig. 1. Micro-computed tomography scans of the skulls of *Calumma nasutum* and *C. radamanus* in dorsal and lateral view. (A) *Calumma nasutum* (MNHN 6643C), male lectotype (with scanning artefact on the jaw bones below the orbit); (B) *C. nasutum* (MNHN 6643), female paralectotype; (C) *C. nasutum* (ZSM 924/2003), male of genetic clade K, assigned to *C. nasutum*; (D) *C. radamanus* (SMF 22132), male holotype; (E) *C. radamanus* (SMF 26394), female paratype; (F) *C. radamanus* (ZSM 475/2010), male of genetic clade GII, assigned to *C. radamanus*. Diagnostic characters are encircled in red. Abbreviations are given in the Material and Methods. Scale bar=2.0 mm.

on the right side. Diagnostic characters are indicated with a greyed number in Table 1. For a better traceability these numbers are also listed in the diagnoses together with the respective characters.

Diagnoses are not provided against each species of the *Calumma boettgeri* group due to their clear identification by their occipital lobes. However, the frontoparietal fenestra (FF), already used as diagnostic character in PRÖTZEL *et al.* (2018b) for the *Calumma boettgeri* complex, is included in the diagnosis because *C. fallax* is known to have a FF in contrast to *C. nasutum* (RIEPEL & CRUMLY, 1997). We structure this paper in dealing first with species with a closed cranial roof, and then with the two species with a significant FF.

We used a Principal Component Analysis (PCA) to verify our assignment of type specimens to species, and to explore the extent of morphological differentiation of species. PCA of external morphology was performed in R 3.5.2 (R CORE TEAM, 2014) using the core STATS package and plotted using GGLOT2 (WICKHAM, 2016). Variables

were scaled against SVL and centred (SVL itself was log-transformed), and adult males and females were analysed separately; subadults and juveniles were excluded.

Micro-CT

For internal morphology, micro-Computed Tomography (micro-CT) scans of the head were prepared for 23 specimens. Specimens were placed in a closed plastic vessel slightly larger than the specimen with the head oriented upwards and stabilized with ethanol-soaked paper. To avoid scanning artefacts, it was ensured that the paper did not cover the head region. Micro-CT scanning was performed with a phoenix|x nanotom m (GE Measurement & Control, Wunstorf, Germany) using a tungsten or diamond target at a voltage of 130 kV and a current of 80 μ A for 29 minutes with 1800 projections à 1000 ms or 15 minutes with 1800 projections à 500 ms. 3D datasets were processed with VG Studio Max 2.2 (Visual

Graphics GmbH, Heidelberg, Germany); the data were visualized using the Phong volume renderer to show the surface of the skull and reflect a variety of different levels of x-ray absorption. The osteological terminology follows RIEPPEL AND CRUMLY (1997). We base our interpretation of skull morphology on volume rendering, following the recommendations of SCHERZ *et al.* (2017). The following skull characters were measured in VG Studio Max 2.2 using the calliper tool, (Fig. 1, Table 2): absence (–) or width of the frontoparietal fenestra (FFW); nasal length (NaL); frontal width measured at prefrontal border (FWPf); frontal width measured at anterior border to postorbitofrontal (FWPo); frontal width measured at frontal-parietal-border (FWPa); parietal width measured at posterior border to postorbitofrontal (PWPo); parietal and squamosal in contact (PSC, +) or not connected (–); parietal width at midpoint (PWm); parietal length (PL); frontal length (FL); snout-casque length, measured from tip of upper jaw to posterior end of parietal (SCL); skull length, measured from tip of upper jaw to skull capsule (SkL); the respective ratios to SkL are indicated with an ‘R’ in front of the character-abbreviations.

Hemipenes of five males, from clade B (ZSM 663/2014), clade GII (ZSM 443/2005), clade H (ZSM 694/2003), clade I (ZSM 1724/2010), and clade K (ZSM 924/2003) were diceCT (diffusible Iodine contrast-enhanced micro-CT) scanned largely following GIGNAC *et al.* (2016). One hemipenis was clipped off from each specimen and immersed in iodine solution (I₂ in 1% ethanol) for seven days to increase X-ray absorbance. For scanning, the hemipenes were placed with their apices oriented upwards in a plastic tube immersed in 70% ethanol. Scanning was performed at a voltage of 60 kV and a current of 200 µA for 18 minutes with 1800 projections à 1000 ms. 3D data were processed in VG Studio Max 2.2 as described above. Hemipenial terminology largely follows KLAVER AND BÖHME (1986) with the addition of the cornucula gemina, a structure named by PRÖTZEL *et al.* (2017). Hemipenes of the remaining males were investigated using a binocular dissecting microscope for consistency and variability.

Genetic analysis

For this study, we used sequences of segments of the mitochondrial gene for NADH dehydrogenase subunit 2 (ND2), and of the nuclear gene for oocyte maturation factor (c-mos) from previous studies (GEHRING *et al.*, 2011, 2012; PRÖTZEL *et al.*, 2017, 2018a, 2018b), and complemented this dataset with sequences of additional samples. Total genomic DNA extraction from tissue samples using proteinase K digestion (10 mg/ml concentration) followed by a salt extraction protocol (BRUFORD *et al.*, 1992). For PCR amplifications we used primers ND2F17 (5'-TGACAAAAAATTGCNCC-3') (MACEY *et al.*, 2000) and ALAR2 (5'-AAAATRTCT-GRGTTGCATTGAC-3') (MACEY *et al.*, 1997) for ND2, and CO8 (5'-CTTGGTGTTCATAGACTGG-3') and

CO9 (5'-TTTGGGAGCATCCAAAGTCTC-3') (HAN *et al.*, 2004) for c-mos. PCR products were purified using ExoSAPIT (USB) and sequenced on automated DNA sequencers. Chromatograms of newly determined DNA sequences were checked for sequencing errors, and absence of frameshifts or stop codons (indicative of pseudogenes) verified in CodonCode Aligner (CodonCode Corporation), and submitted to GenBank (accession numbers MN107761–MN107848).

Our sampling includes all available ND2 and c-mos sequences, plus complementary new sequences, for all species of the *Calumma nasutum* group sensu lato, i.e., all small Malagasy chameleon species with soft dermal flaps on their snout tips. Phylogenetic analyses have suggested that this group might be paraphyletic with respect to the species of the *C. brevicorne* group (TOLLEY *et al.*, 2013), but clarifying this question is beyond the scope of the present study. As discussed below, all species of the *C. brevicorne* group can be easily distinguished morphologically by the absence of a dermal snout flap, and for the purpose of taxonomic revision herein, their omission is therefore justified.

Sequences were aligned in MEGA7 (KUMAR *et al.*, 2016). We used the ND2 alignment (582 bp) in a Maximum Likelihood (ML) phylogenetic analysis under a GTR + G model as selected by the Bayesian Information Criterion implemented in MEGA7. 500 full heuristic bootstrap replicates were run in MEGA7, with subtree-pruning-regrafting (SPR level 5) branch swapping. A sequence of *Calumma oshaughnessyi* (Günther, 1881) was used as an outgroup.

In our species delimitation rationale, we rely on concordance of the differentiation in mitochondrial DNA represented by the ND2 gene, with differentiation in the nuclear c-mos gene. Therefore, the c-mos sequences (360 bp) were analysed independently. We first separated c-mos sequences into haplotypes using the Phase algorithm (STEPHENS *et al.*, 2001) as implemented in DNAsp 5 (LIBRADO & ROZAS, 2009). We then used the phased sequences to construct a haplotype network following the approach of SALZBURGER *et al.* (2011) with the program Haplotype Viewer (<http://www.cibiv.at/~greg/haploviewer>) based on an ML tree reconstructed in MEGA7 under the Jukes Cantor substitution model.

Results

Genetic differentiation in the *Calumma nasutum* group

The ML analysis of ND2 sequences of 303 individuals of the *C. nasutum* group provided a tree (Fig. 2) largely in agreement with that of GEHRING *et al.* (2012). All species recognized by GEHRING *et al.* (2012) and described in subsequent studies formed monophyletic groups. In addition, the tree also contains various other deep clades

Table 2. Osteological measurements of the *Calumma nasutum* group. f, female; m, male; further abbreviations see Material and Methods; all measurements are in millimetres.

species	collection no.	sex	FFW	RFFD	NaL	RNaL	FWPF	RFWPF	FWPo	RFWPo	FWPa	RFWPa	PWPo	RPWPo
			14											
<i>C. nasutum</i>	MNHN 6643C	m	—	—	1.6	13.0%	2.4	19.5%	4.9	39.8%	4.2	34.1%	5.0	40.7%
<i>C. nasutum</i>	MNHN 6643B	m	—	—	1.9	15.6%	2.5	20.5%	3.7	30.3%	3.8	31.1%	4.0	32.8%
<i>C. nasutum</i>	ZSM 924/2003	m	—	—	1.8	15.4%	2.8	23.9%	4.3	36.8%	3.6	30.8%	3.5	29.9%
<i>C. nasutum</i>	MNHN 6643	f	—	—	1.9	14.7%	2.5	19.4%	4.1	31.8%	4.0	31.0%	4.3	33.3%
<i>C. nasutum</i>	ZSM 1699/2012	f	—	—	1.9	16.2%	2.4	20.5%	3.8	32.5%	3.6	30.8%	3.7	31.6%
<i>C. emelinae</i> sp. nov.	ZSM 618/2009	m	—	—	1.7	14.5%	3.0	25.6%	4.4	37.6%	3.9	33.3%	4.2	35.9%
<i>C. fallax</i>	MNHN 1899.317	m	2.4	20.0%	1.8	15.0%	2.7	22.5%	4.4	36.7%	3.6	30.0%	3.9	32.5%
<i>C. fallax</i>	MNHN 1890.430	m	2.3	19.0%	1.7	14.0%	3.1	25.6%	4.5	37.2%	3.7	30.6%	3.8	31.4%
<i>C. fallax</i>	ZSM 693/2003	m	2.1	18.6%	2.5	22.1%	2.3	20.4%	4.3	38.1%	3.5	31.0%	3.4	30.1%
<i>C. fallax</i>	ZSM 286/2010	m	2.2	17.3%	1.7	13.4%	3.3	26.0%	4.8	37.8%	4.0	31.5%	4.2	33.1%
<i>C. ratnasariae</i> sp. nov.	ZSM 35/2016	m	2.5	21.0%	2.0	16.8%	2.6	21.8%	4.4	37.0%	3.8	31.9%	4.0	33.6%
<i>C. ratnasariae</i> sp. nov.	ZSM 517/2014	m	2.2	18.6%	2.0	16.9%	2.0	16.9%	4.3	36.4%	3.7	31.4%	4.2	35.6%
<i>C. tjiasmantoi</i> sp. nov.	ZSM 735/2003	f	—	—	2.1	16.9%	2.4	19.4%	4.3	34.7%	3.8	30.6%	4.3	34.7%
<i>C. radamanus</i>	SMF 22132	m	—	—	1.8	15.1%	3.4	28.6%	4.8	40.3%	3.7	31.1%	4.0	33.6%
<i>C. radamanus</i>	ZSM 619/2009	m	—	—	1.6	13.8%	2.7	23.3%	4.9	42.2%	4.0	34.5%	4.1	35.3%
<i>C. radamanus</i>	ZSM 475/2010	m	—	—	2.1	17.8%	3.0	25.4%	4.5	38.1%	4.0	33.9%	3.4	28.8%
<i>C. radamanus</i> complex	ZSM 145/2016	m	—	—	1.6	12.9%	2.6	21.0%	4.5	36.3%	4.1	33.1%	4.6	37.1%
<i>C. radamanus</i> complex	ZSM 1694/2012	m	—	—	1.3	11.1%	2.4	20.5%	4.5	38.5%	4.0	34.2%	4.6	39.3%
<i>C. radamanus</i> complex	ZSM 1691/2012	m	—	—	1.7	13.5%	3.0	23.8%	4.8	38.1%	4.1	32.5%	4.5	35.7%
<i>C. radamanus</i> complex	ZSM 441/2005	m	—	—	1.9	15.8%	2.2	18.3%	4.0	33.3%	4.0	33.3%	4.3	35.8%
<i>C. radamanus</i> complex	ZSM 88/2015	f	—	—	1.8	15.0%	2.0	16.7%	4.1	34.2%	3.9	32.5%	4.3	35.8%
<i>C. volhibola</i>	ZSM 645/2009	m	—	—	2.0	17.2%	2.2	19.0%	3.9	33.6%	3.5	30.2%	4.0	34.5%

species	collection no.	sex	PSC	PWm	RPWm	PL	RPL	FL	RFL	SCL	RSCL	SkL
			15	16	16							
<i>C. nasutum</i>	MNHN 6643C	m	+	1.2	9.8%	5.3	43.1%	6.3	51.2%	15.6	126.8%	12.3
<i>C. nasutum</i>	MNHN 6643B	m	+	1.4	11.5%	5.4	44.3%	9.6	78.7%	14.5	118.9%	12.2
<i>C. nasutum</i>	ZSM 924/2003	m	+	1.9	16.2%	4.8	41.0%	9.6	82.1%	13.7	117.1%	11.7
<i>C. nasutum</i>	MNHN 6643	f	+	1.8	14.0%	5.6	43.4%	7.1	55.0%	15.2	117.8%	12.9
<i>C. nasutum</i>	ZSM 1699/2012	f	+	2.1	17.9%	4.1	35.0%	6.0	51.3%	13.0	111.1%	11.7
<i>C. emelinae</i> sp. nov.	ZSM 618/2009	m	+	1.9	16.2%	4.8	41.0%	6.5	55.6%	13.8	117.9%	11.7
<i>C. fallax</i>	MNHN 1899.317	m	+	0.8	6.7%	4.3	35.8%	5.4	45.0%	14.6	121.7%	12.0
<i>C. fallax</i>	MNHN 1890.430	m	+	1.9	15.7%	5.2	43.0%	6.1	50.4%	15.2	125.6%	12.1
<i>C. fallax</i>	ZSM 693/2003	m	—	1.3	11.5%	3.8	33.6%	5.7	50.4%	13.6	120.4%	11.3
<i>C. fallax</i>	ZSM 286/2010	m	+	1.6	12.6%	4.9	38.6%	5	39.4%	15.8	124.4%	12.7

Table 2 continued.

species	collection no.	sex	PSC	PWm	RPWm	PL	RPL	FL	RFL	SCL	RSCL	SkL
<i>C. ratnasariae</i> sp. nov.	ZSM 35/2016	m	+	2.2	18.5%	4.2	35.3%	5.5	46.2%	14.4	121.0%	11.9
<i>C. ratnasariae</i> sp. nov.	ZSM 517/2014	m	+	2.1	17.8%	3.8	32.2%	5.5	46.6%	13.9	117.8%	11.8
<i>C. tjasamantoi</i> sp. nov.	ZSM 735/2003	f	+	2.0	16.1%	4.5	36.3%	6.2	50.0%	14.4	116.1%	12.4
<i>C. radamanus</i>	SMF 22132	m	—	2.3	19.3%	4.8	40.3%	6.7	56.3%	14.1	118.5%	11.9
<i>C. radamanus</i>	ZSM 619/2009	m	—	2.6	22.4%	4.7	40.5%	6.5	56.0%	13.8	119.0%	11.6
<i>C. radamanus</i>	ZSM 475/2010	m	—	1.9	16.1%	4.4	37.3%	6.7	56.8%	13.5	114.4%	11.8
<i>C. radamanus</i> complex	ZSM 145/2016	m	—	2.8	22.6%	5.0	40.3%	6.8	54.8%	14.8	119.4%	12.4
<i>C. radamanus</i> complex	ZSM 451/2016	m	—	1.7	16.2%	3.9	37.1%	5.9	56.2%	12.2	116.2%	10.5
<i>C. radamanus</i> complex	ZSM 1694/2012	m	—	2.8	23.9%	5.5	47.0%	6.8	58.1%	14.8	126.5%	11.7
<i>C. radamanus</i> complex	ZSM 1691/2012	m	—	2.4	19.0%	5.1	40.5%	6.5	51.6%	15.3	121.4%	12.6
<i>C. radamanus</i> complex	ZSM 441/2005	m	—	2.2	18.3%	5.3	44.2%	6.1	50.8%	14.8	123.3%	12.0
<i>C. radamanus</i> complex	ZSM 88/2015	f	—	1.7	14.2%	4.7	39.2%	6.6	55.0%	13.5	112.5%	12.0
<i>C. vohibola</i>	ZSM 645/2009	m	+	1.6	13.8%	4.6	39.7%	5.6	48.3%	13.6	117.2%	11.6

already recognized by GEHRING *et al.* (2012) and not yet taxonomically resolved, i.e., clades B, G, H, I, J, and K. All of these clades received substantial bootstrap support of usually > 90% (Fig. 2) in the mitochondrial analyses, and they are characterized by high ND2 divergences to each other and to the taxonomically well-understood species (Table 3). Mean uncorrected pairwise distances ranged from 9.1% between *C. guibei* and *C. lefona*, to 20.5% between *C. boettgeri* and *C. guibei*. However, substantial genetic divergences were also found within species and main clades, as discussed previously (GEHRING *et al.*, 2012; PRÖTZEL *et al.*, 2017, 2018b). Intra-clade pairwise distances amounted to 11.6% in clade G and in *C. gehringi*, 11.8% in clade H, and 12.2% in *C. gallus* (clade A).

A haplotype network based on *c-mos* sequences of 114 individuals of the *C. nasutum* group revealed that most of the recognized species and taxonomically unresolved deep mitochondrial clades also show divergence in this nuclear gene (Fig. 3). Haplotype sharing was exceedingly rare and only observed between *C. vohibola* and clade B, although in some other species and clades, the reconstructed haplotypes did not form clearly delimited phylogroups (clade I, clade J).

General diagnosis of the *Calumma nasutum* group to all other chameleons

All species described or re-described in the following belong to the phenetic *Calumma nasutum* species group. Therefore, a general delimitation of the *C. nasutum* group to the other Chameleoninae from Madagascar is provided here: The phenetic *Calumma nasutum* group comprises small species, with a total length of about 80–130 mm, usually bearing a soft dermal appendage on the snout tip (Fig. 4). Species of the genus *Furcifer* are larger and their rostral processes, if present at all, are of bony origin. The smallest species, *F. campani* with a maximum TL of 135 mm (GLAW & VENCES, 2007), lacks a rostral appendage. In *Calumma* only species of the *C. furcifer* group – defined in GLAW AND VENCES (1994) – are of similar size and morphology. However, the *C. nasutum* group differs from them by a heterogeneous scalation on the extremities (vs homogeneous), a lower number of supra- and infralabials, and a shorter snout; for more details and measurements, see PRÖTZEL *et al.* (2016). Furthermore we revise the assignment of *C. peyrierasi*, which was assigned to this group in PRÖTZEL *et al.* (2016), and exclude the species again from the *C. nasutum* group, since it lacks most of the features that characterize the group (soft rostral appendage, heterogeneous scalation on the extremities, etc.), is larger, and has a differently shaped casque (data not shown). Its assignment remains unclear, but will be revised in future work on the phylogeny of *Calumma*.

Within the *C. nasutum* group eight species, *C. boettgeri* (Boulenger, 1888), *C. gehringi* Prötzel *et al.*, 2017, *C. guibei* (Hilgenius, 1959), *C. juliae* Prötzel *et al.*, 2018, *C. lefona* Prötzel *et al.*, 2018, *C. linotum* (Müller, 1924), *C. roaloko* Prötzel *et al.*, 2018, and *C. uetzi* Prötzel *et al.*, 2018 differ from the others by the possession of well-defined occipital lobes and are referred to as the *C. boettgeri* complex (whose monophyly is uncertain, as is the monophyly of the entire *C. nasutum* group). *Calumma gallus* (Günther, 1877), which lacks occipital lobes and is characterized by a long, pointed rostral appendage of 5–11 mm length in

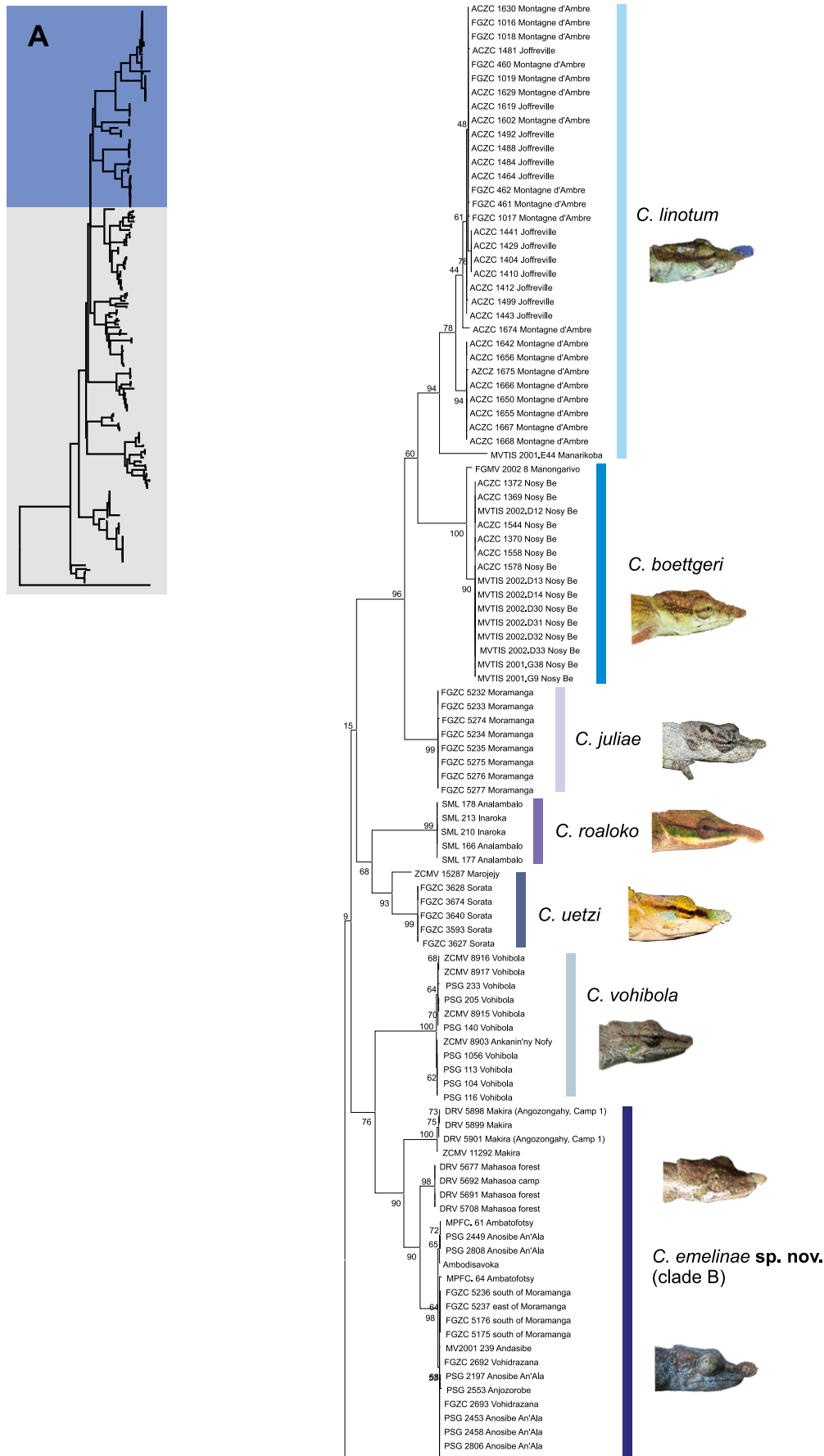


Fig. 2. Maximum likelihood tree based on DNA sequences of the mitochondrial ND2 gene (582 bp) of species of the *Calumma nasutum* group. Numbers at nodes are bootstrap proportions expressed as a percentage (500 replicates). Tip labels are field numbers followed by collection locality. Note: *Calumma lefona* was listed with a wrong field number (DRV 6284) in Fig. 1 of Prötzel *et al.* (2018b) and in Fig. 2 of Prötzel *et al.* (2018a).

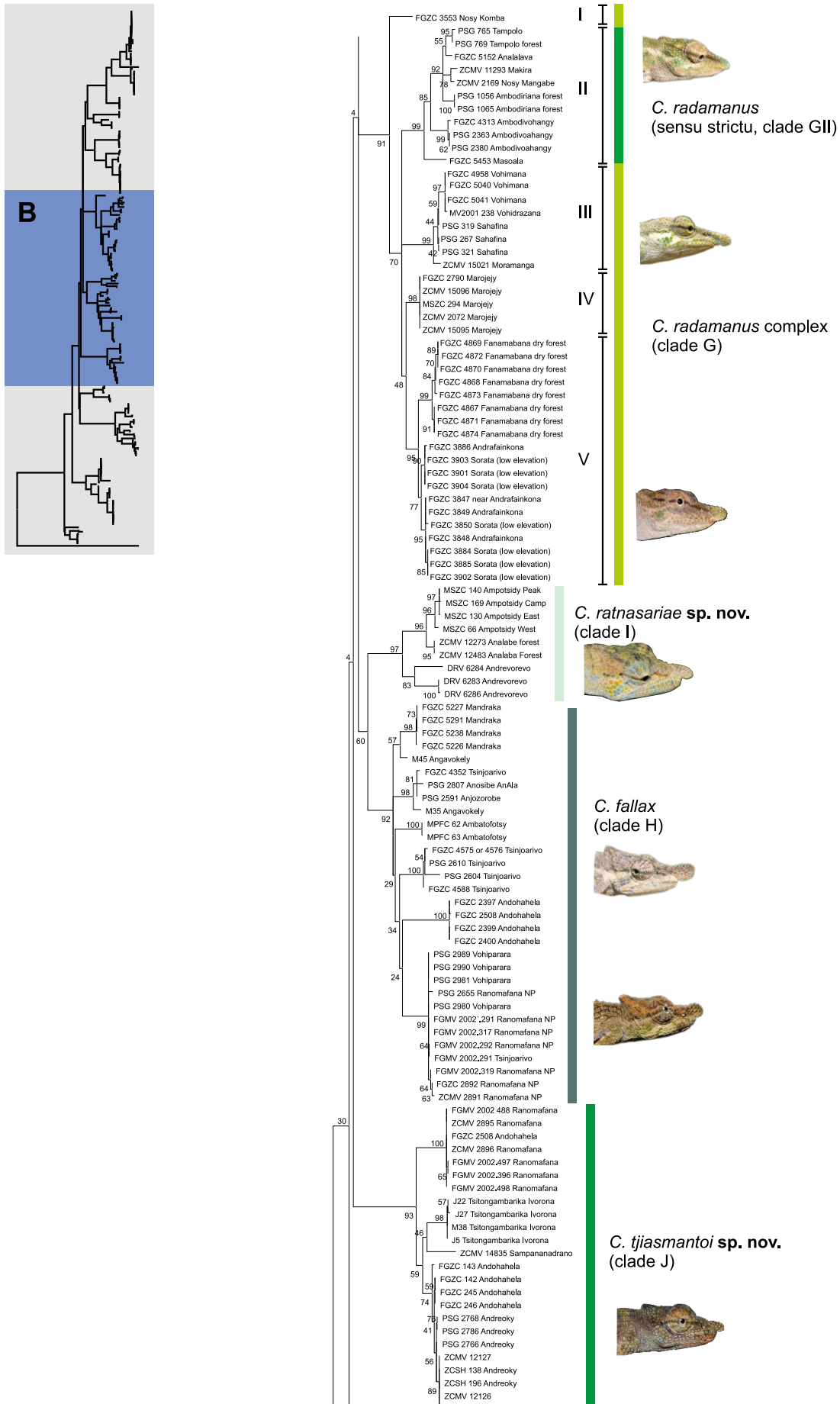


Fig. 2 continued.

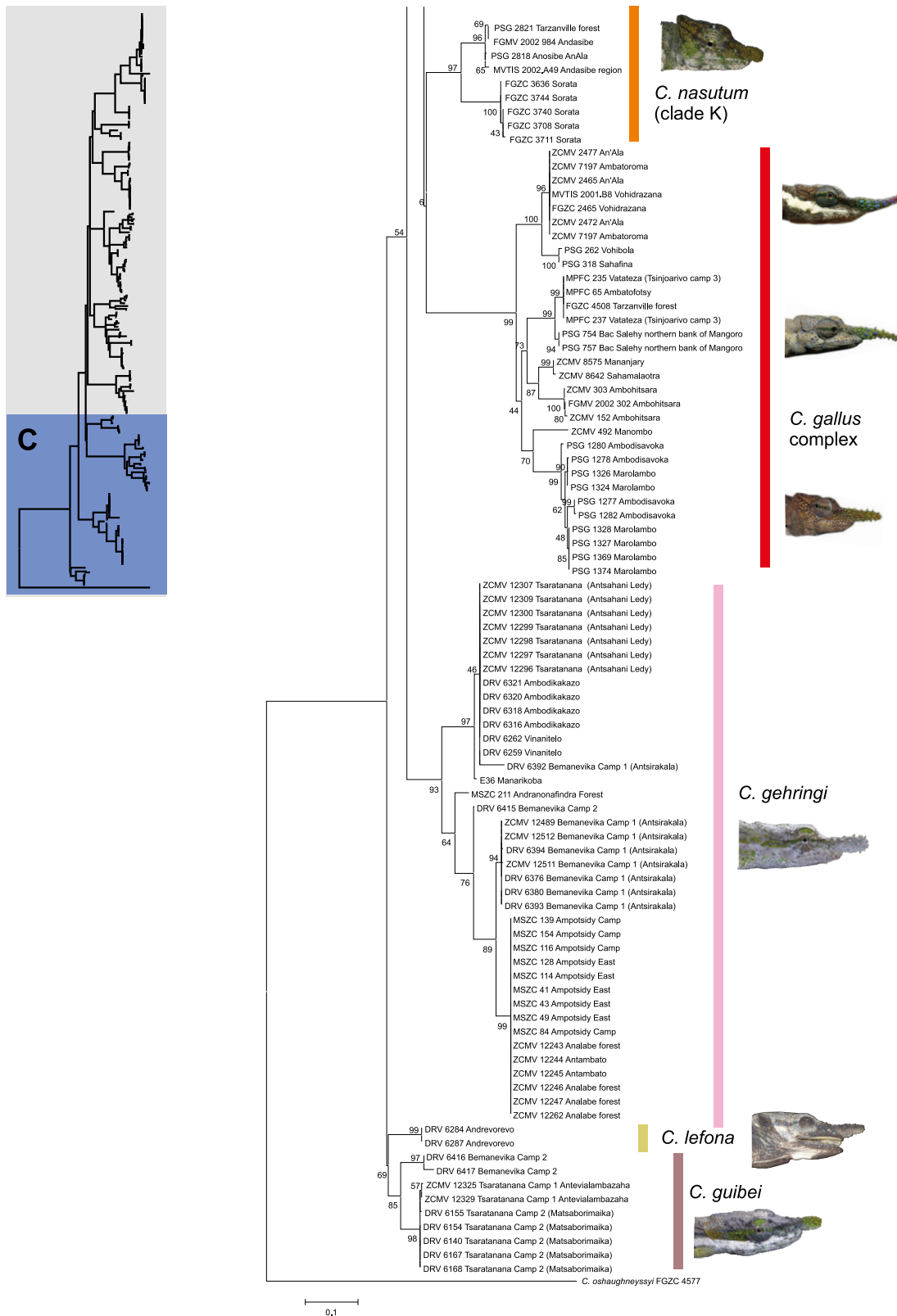


Fig. 2 continued.

males and a short and rounded appendage of distinct red colour in females (GLAW & VENCES, 2007), constitutes a separate species complex; clade A in GEHRING *et al.* (2012). The taxonomy of *C. gallus* is in need of revision and will be treated elsewhere. Including the remaining

species *C. fallax* (Mocquard, 1900), *C. nasutum* (Duméril & Bibron, 1836), *C. vatosoa* Andreone, Mattioli, Jesu & Randrianirina, 2001, and *C. vohibola* Gehring, Ratsoavina, Vences & Glaw, 2011, the *C. nasutum* group at present contains 13 described species.

Table 3. Mean uncorrected pairwise distances (in percent) between species of the *Calumma nasutum* group for a segment of the ND2 gene. The grey cells show mean distances within species.

	<i>C. boettgeri</i>	<i>C. emelinae</i> sp. nov.	<i>C. fallax</i>	<i>C. gallus</i>	<i>C. gehringi</i>	<i>C. guibei</i>	<i>C. juliae</i>	<i>C. lefona</i>	<i>C. linotum</i>	<i>C. nasutum</i>	<i>C. radamanus</i>	<i>C. ratnasariae</i> sp. nov.	<i>C. roaloko</i>	<i>C. tjiasmantoi</i> sp. nov.	<i>C. uetzi</i>	<i>C. vohibola</i>	
<i>C. boettgeri</i>	0.2																
<i>C. emelinae</i> sp. nov.	18.5	3.6															
<i>C. fallax</i>	17.5	13.9	7.2														
<i>C. gallus</i>	19.1	17.4	17.3	8.5													
<i>C. gehringi</i>	16.4	13.6	15.1	17.4	6.2												
<i>C. guibei</i>	20.5	15.4	14.8	16.2	14.5	2.7											
<i>C. juliae</i>	11.4	14.6	14.7	16.8	12.8	15.2	0.0										
<i>C. lefona</i>	18.4	15.0	14.8	16.1	14.1	9.1	14.5	0.0									
<i>C. linotum</i>	12.6	13.6	14.8	17.5	15.0	16.7	11.0	14.5	2.1								
<i>C. nasutum</i>	15.8	13.4	14.1	16.3	13.0	14.1	13.3	13.4	13.4	4.5							
<i>C. radamanus</i>	18.8	14.5	14.5	16.0	14.1	14.5	15.7	13.7	15.1	13.5	7.2						
<i>C. ratnasariae</i> sp. nov.	19.1	15.3	13.3	18.1	15.3	15.9	14.7	15.6	15.3	15.0	15.3	6.4					
<i>C. roaloko</i>	17.9	14.2	14.6	17.2	15.3	15.3	13.6	13.9	14.5	14.8	14.7	15.7	0.1				
<i>C. tjiasmantoi</i> sp. nov.	16.7	14.6	14.7	16.9	14.6	15.8	14.9	15.9	15.3	14.0	14.5	15.3	16.6	4.7			
<i>C. uetzi</i>	15.3	12.4	12.8	15.9	12.4	14.7	12.8	13.6	12.2	12.9	12.8	13.3	11.9	13.3	2.4		
<i>C. vohibola</i>	19.3	12.4	15.4	18.0	14.5	15.8	14.6	15.4	15.5	15.0	15.6	15.2	15.4	14.9	12.1	0.4	

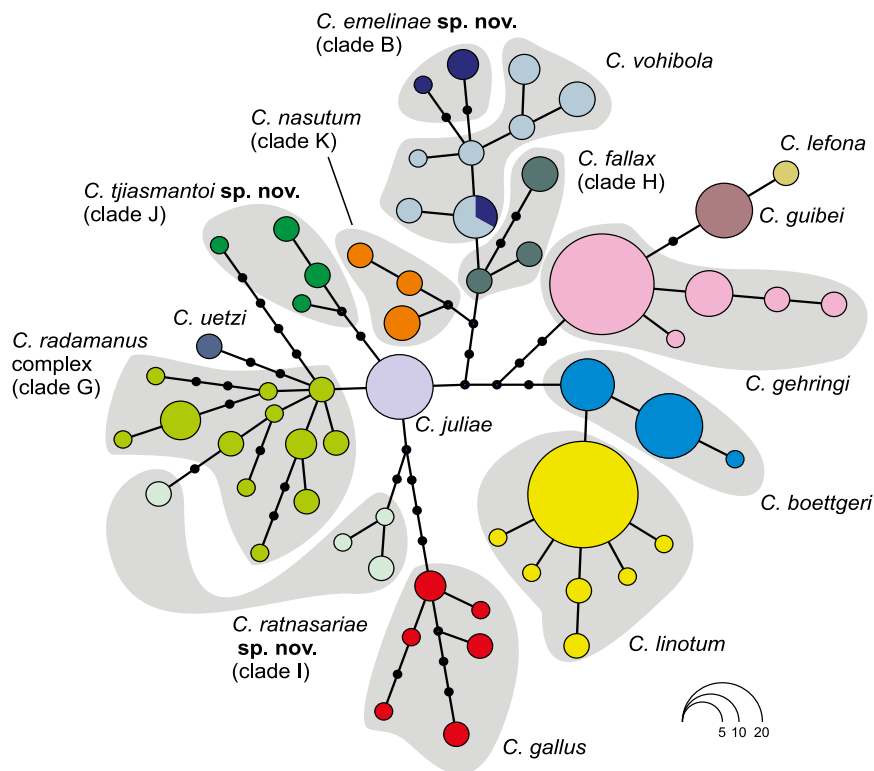


Fig. 3. Haplotype network estimated from sequences of the nuclear *c-mos* gene (360 bp). Black dots represent additional mutational steps. The size of a coloured circle correlates with the sample number, see scale.

Hemipenis morphology of the *Calumma nasutum* group (Fig. 5)

The genital morphology within the group is conserved and differs only in a few characters between species. Therefore, a description of the general morphology is

provided here and only specific characters are listed in the respective species descriptions.

The general form of the hemipenis of the *Calumma nasutum* group is subcylindrical and symmetrical with a slightly bilobed apex; calyces on the truncus are distinct and clearly reduced on the sulcal side, but similar on the upper truncus and pedicel (the *C. gallus* complex

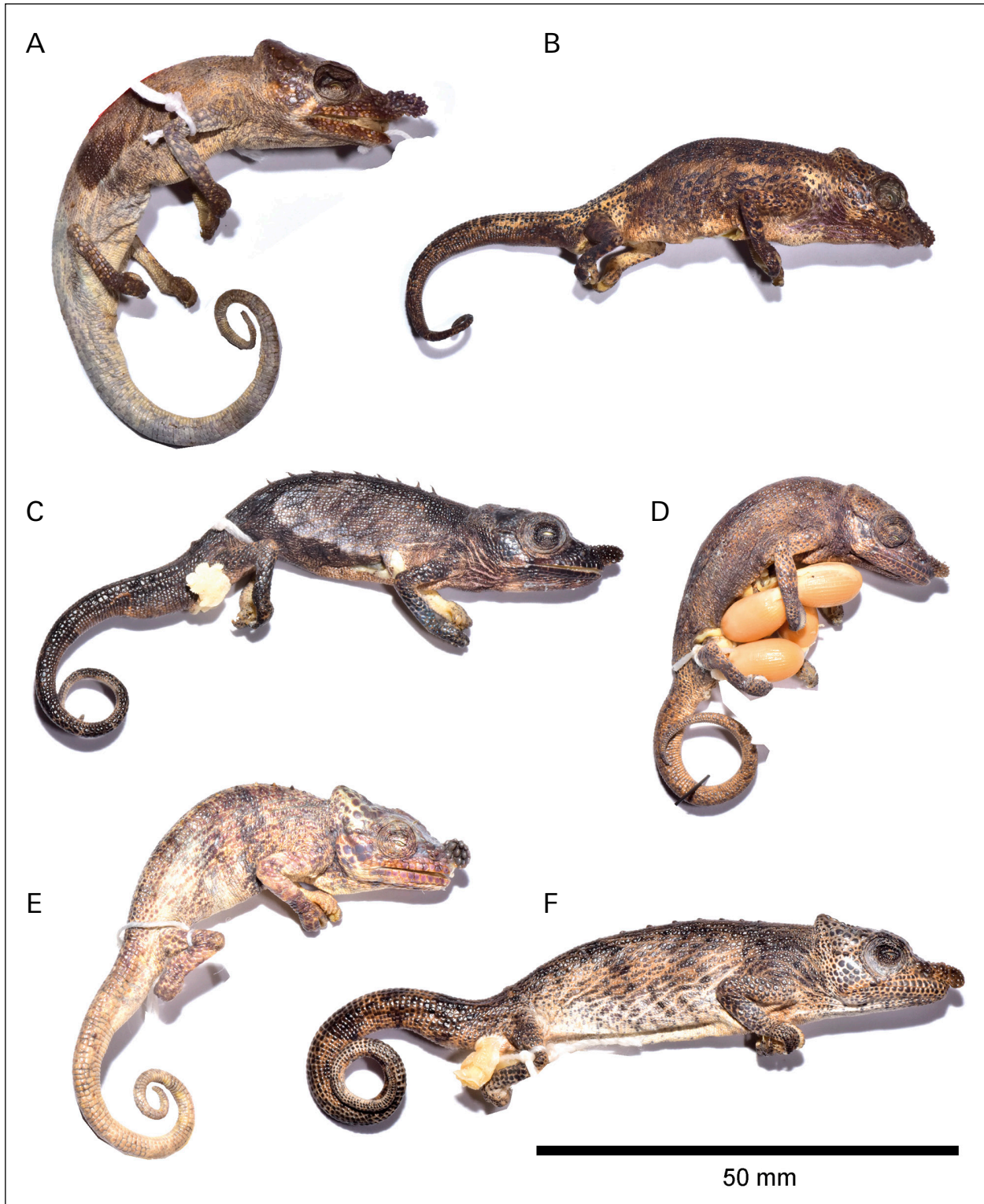


Fig. 4. Preserved type specimens of (A) *Calumma nasutum* (lectotype, MNHN 6643C), adult male; (B) *C. radamanus* (holotype, SMF 22132), adult male; (C) *C. emelinae* sp. nov. (holotype, ZSM 618/2009), adult male; (D) *C. tjiasmantoi* sp. nov. (holotype, ZSM 735/2003), adult female; (E) *C. fallax* (lectotype, MNHN 1899.317), adult male; (F) *C. ratnasariae* sp. nov. (ZSM 35/2016), adult male.

has reduced calyces on the pedicel), size of calyces can differ (hemipenial character A); calyx ridges are smooth and not serrated; two pairs of rotulae that are finely denticulated; both pairs of rotulae can be small, or one pair can be larger than the other (hemipenial character B); between the rotulae a papillary field of small, unpaired pa-

pillae can be present or absent (hemipenial character C); a pair of cornucula gemina, as defined in PRÖTZEL *et al.* (2017), rising from the sulcal side and curved to the asulcal side can be present or absent (hemipenial character D); no other ornaments (e.g. fleshy papillae, horns, pedunculi) occur in this species group.

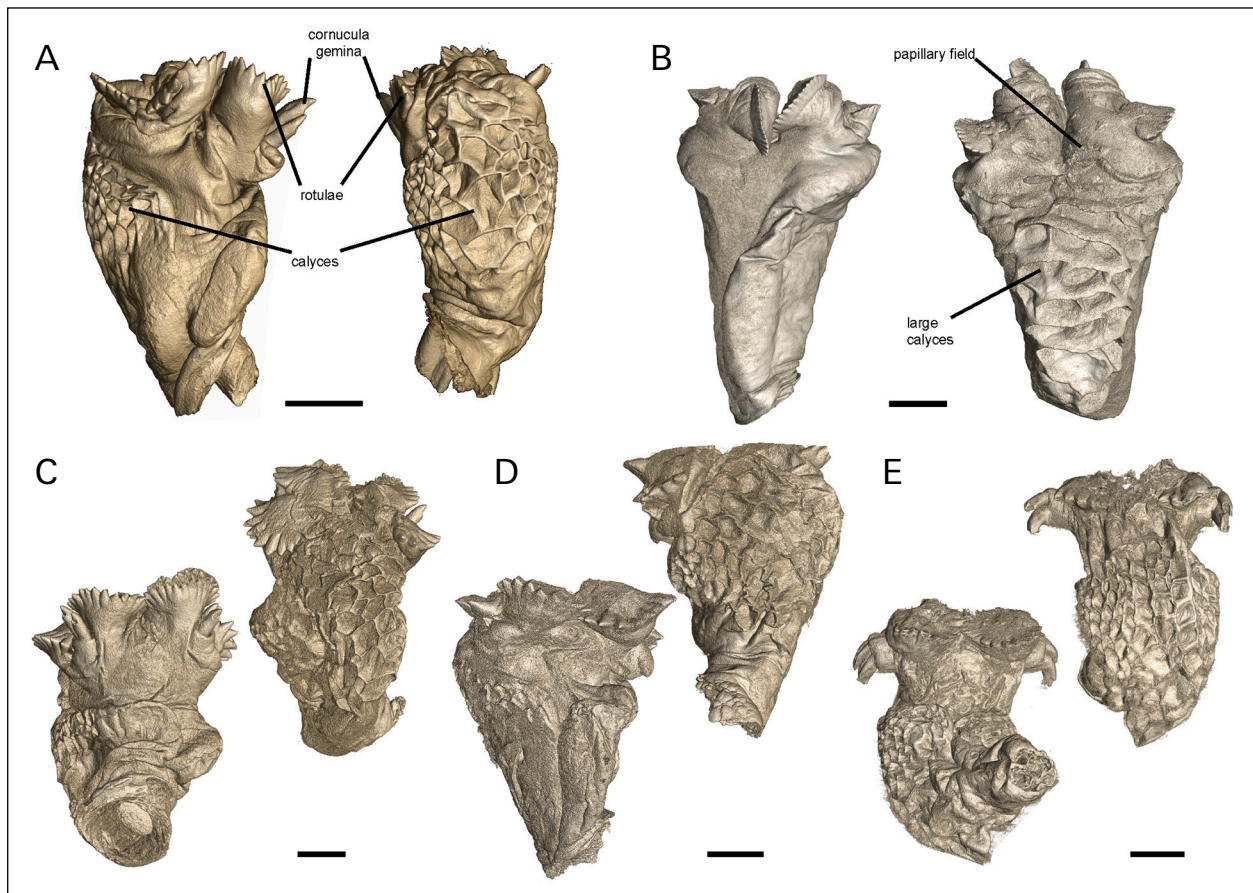


Fig. 5. Micro-CT scans of hemipenes of representative males of the different new or redescribed *Calumma* species (as far as available), each in sulcal (left) and asulcal or lateral view (right). (A) *C. fallax* (ZSM 694/2003); (B) *C. radamanus* (ZSM 443/2005); (C) *C. emelinae* sp. nov. (ZSM 618/2009); (D) *C. nasutum* (ZSM 924/2003); (E) *C. ratnasariae* sp. nov. (ZSM 1724/2010). Scale bar = 1 mm.

Morphological PCA of the *Calumma nasutum* group (Fig. 6)

Principal Component Analysis (PCA) of the external morphology (size-corrected measurements, meristics, and binary characters) of males (Fig. 6B) and females (Fig. 6A) shows clustering of specimens by genetic clades, and specimens assigned to these clades based on our taxonomic revision below. Considerable overlap exists between some clades, such as K and B, and H and I, but certain distinctions are worth noting, especially those that pertain to the existing names *C. nasutum*, *C. radamanus*, and *C. fallax*. In Fig. 6, we have anticipated our taxonomic conclusions below by already including type specimens, including newly designated lectotypes, within the hulls of different clades.

PCA shows that the lectotype of *C. fallax* that we designate below (MNHN 1899.317) fits the overall morphology of clade H. It is generally distinct from clade K, which is below assigned to *C. nasutum*. Clades K and H show no overlap in a plot of the first and second principal components (PCs) for females, and relatively little overlap in PC1 vs PC2 for males. This result shows that there is a moderately consistent distinction between these two forms. Additional osteological characters (especially the

presence of a frontoparietal fenestra) further strengthen the distinction of these two clades (see the re-descriptions of *C. nasutum* and *C. fallax*, below).

In both males and females, the G clade shows strong distinction from all other members of the *C. nasutum* complex (Fig. 6A,B), a distinction arising primarily due to relative tail length and the upper margin of the supralabial scales, together with the number of supralabials and, in females, infralabials. The holotype of *C. radamanus* (SMF 22132) falls clearly within the G clade cluster morphologically. Clade GII is not strongly differentiated from other G subclades, but this may be due to small sample sizes of the respective subclades. The male lectotype of *C. nasutum* that we designate below (MNHN 6643C) falls separately from clade G (Fig. 6B), but is also not clearly within any other cluster. However, based on additional characters from osteology, we below assign it to clade K, which is clearly distinct from clade G.

Identity and re-description of *Calumma nasutum* (Duméril & Bibron, 1836)

For a synonymy list of *C. nasutum*, see GLAW (2015). We here consider *C. radamanus* as a valid species, and resurrect it below with a full justification.

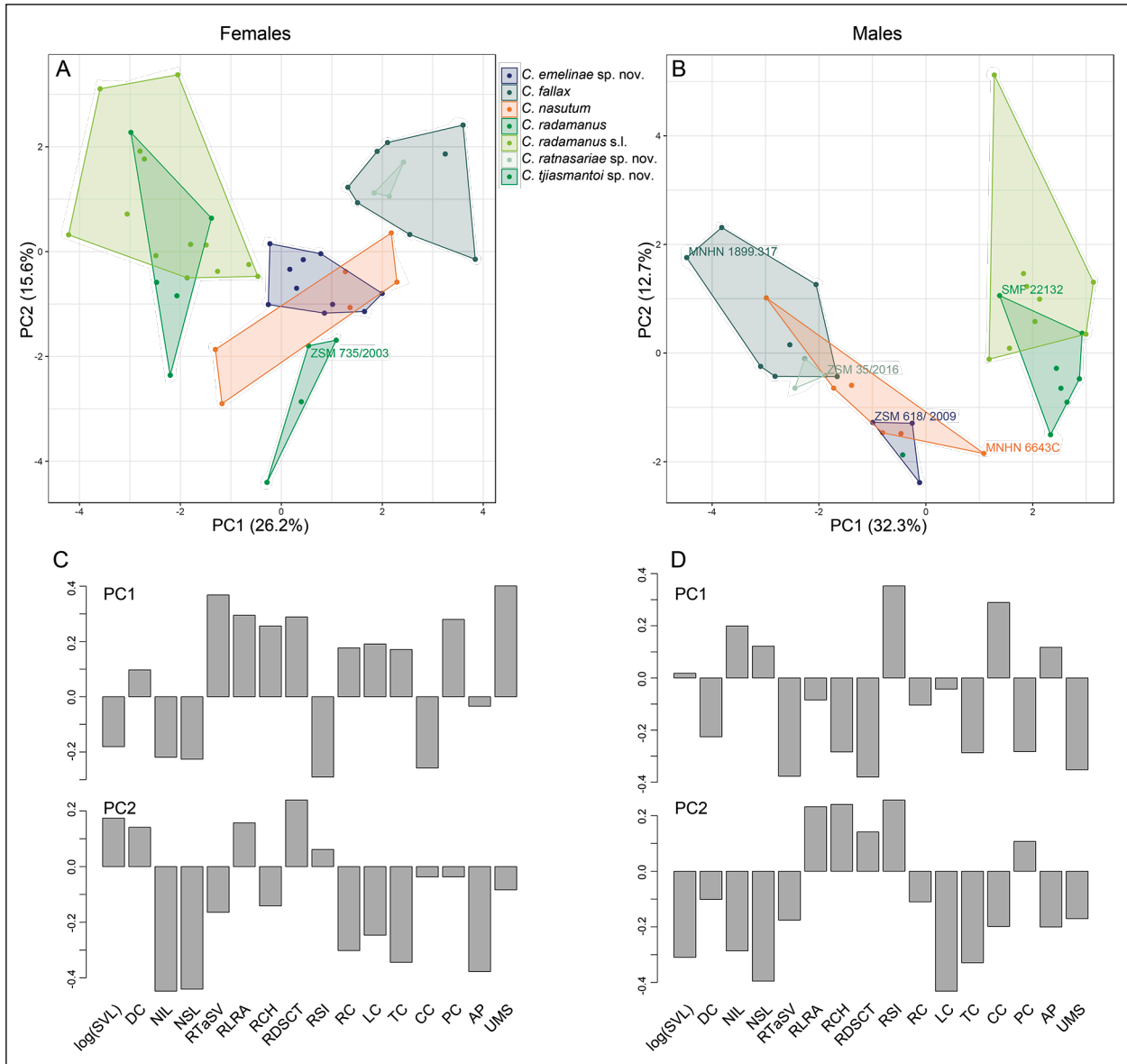


Fig. 6. Principal Component Analysis of morphology within the *Calumma nasutum* species complex. Females (A and C) were analysed separately from males (B and D). C and D show loadings for the respective first and second principal components. Specimen numbers are shown for holotypes and lectotypes of the respective species as described or re-defined herein. Colours correspond to those used in Fig. 2.

Syntypes: Following DUMÉRIL AND BIBRON (1836) as well as KLAVER AND BÖHME (1997) and GEHRING *et al.* (2011), we consider the syntypes of the species to be MNHN 6643 (no field number), adult female, MNHN 6643A (1994/608), adult female, MNHN 6643B (1994/609), adult male, and MNHN 6643C (1994/610), adult male, collected by Alphonse Charles Bernier, with the type locality ‘Madagascar’. Additional material that was considered to be part of this series by MOCQUARD (1900b) (five additional specimens) are not among the four types mentioned by DUMÉRIL AND BIBRON (1836) and therefore are here considered referred material.

Identity of the type specimens: Bernier collected plants, insects, lemurs, reptiles, and birds in Madagascar, and also plants in Réunion (DORR, 1997). Species collected by him and named after him are distributed all over

Madagascar (e.g. the snake species *Dromicodryas bernieri* (DUMÉRIL *et al.*, 1854) and a couple of bird and plant species), so no clear conclusions about the collection locality of the *C. nasutum* type specimens can be drawn. However, only a few rainforest regions were accessible on Madagascar at that time, and two areas are the most likely sources of the specimens: Nosy Be, an island off the north-western coast of Madagascar, and the National Road between the capital Antananarivo and Toamasina (Tamatave) on the east coast, which passes through the rainforests of the Moramanga-Andasibe region. As discussed below, the type series morphologically most closely resembles specimens of clade K, and differs from specimens of clade B in a number of characters. Clade K is known from the vicinity of Andasibe and from Sorata in northern Madagascar. We tentatively conclude that the Andasibe region is the likely source of the type series.

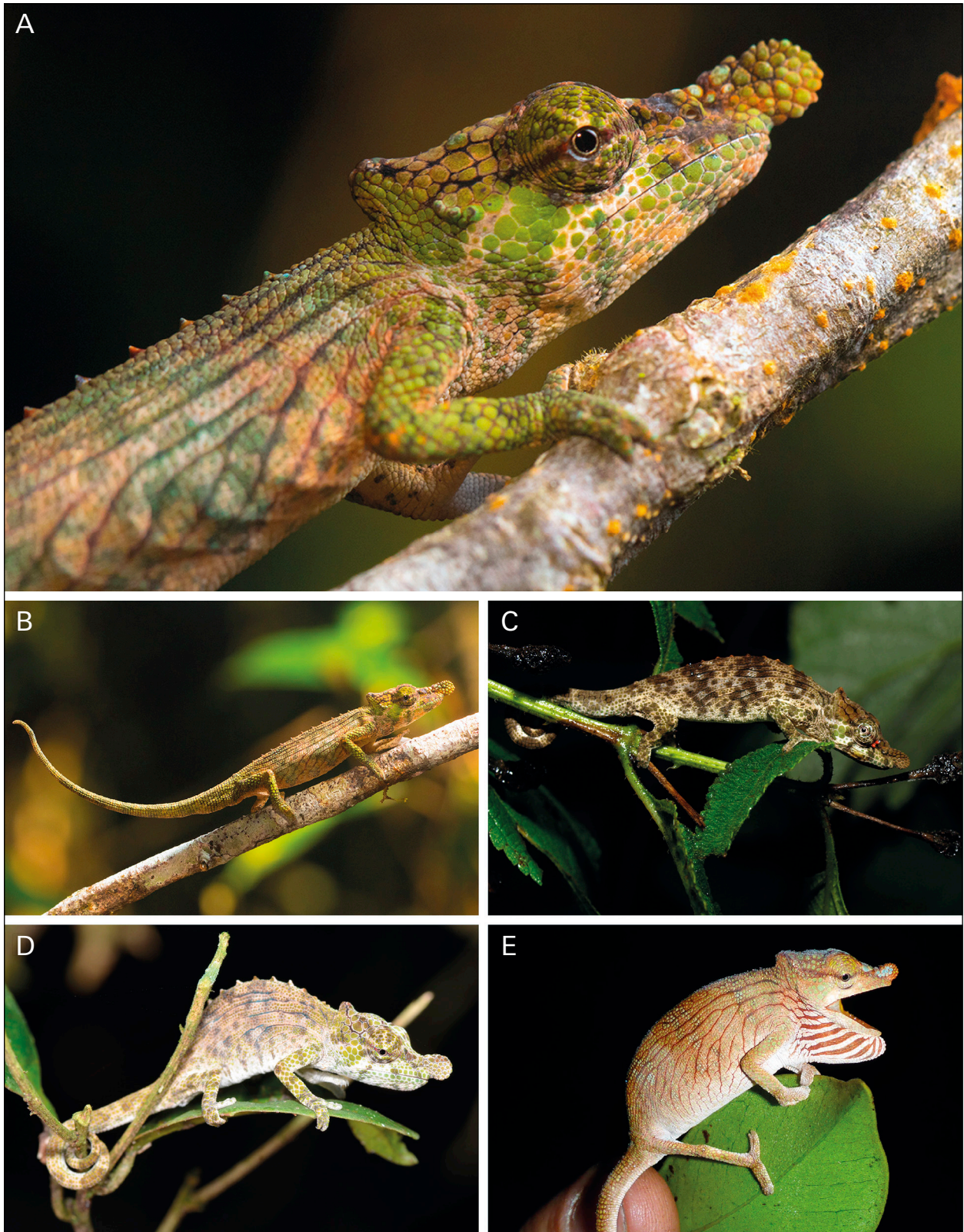


Fig. 7. *Calumma nasutum* (clade K) in life from Andasibe region. (A, B) adult male (not collected) from Mitsinjo/Andasibe in relaxed state, photo: T. Negro/A. Laube; (C) adult male (not collected) from Andasibe in stressed colouration, photo: P-S. Gehring; (D) juvenile male from Maromizaha Reserve (ZSM 256/2016), slightly stressed; (E) juvenile female (not collected) from Maromizaha, in stressed colouration.

Our assignment to the genetic clade K is based on comparison of male syntypes MNHN 6643C (1994/610; below designated as the lectotype) and MNHN 6643B

(1994/609; paralectotype) with two available males (with only one male sequenced and the other morphologically and geographically assigned to clade K): the

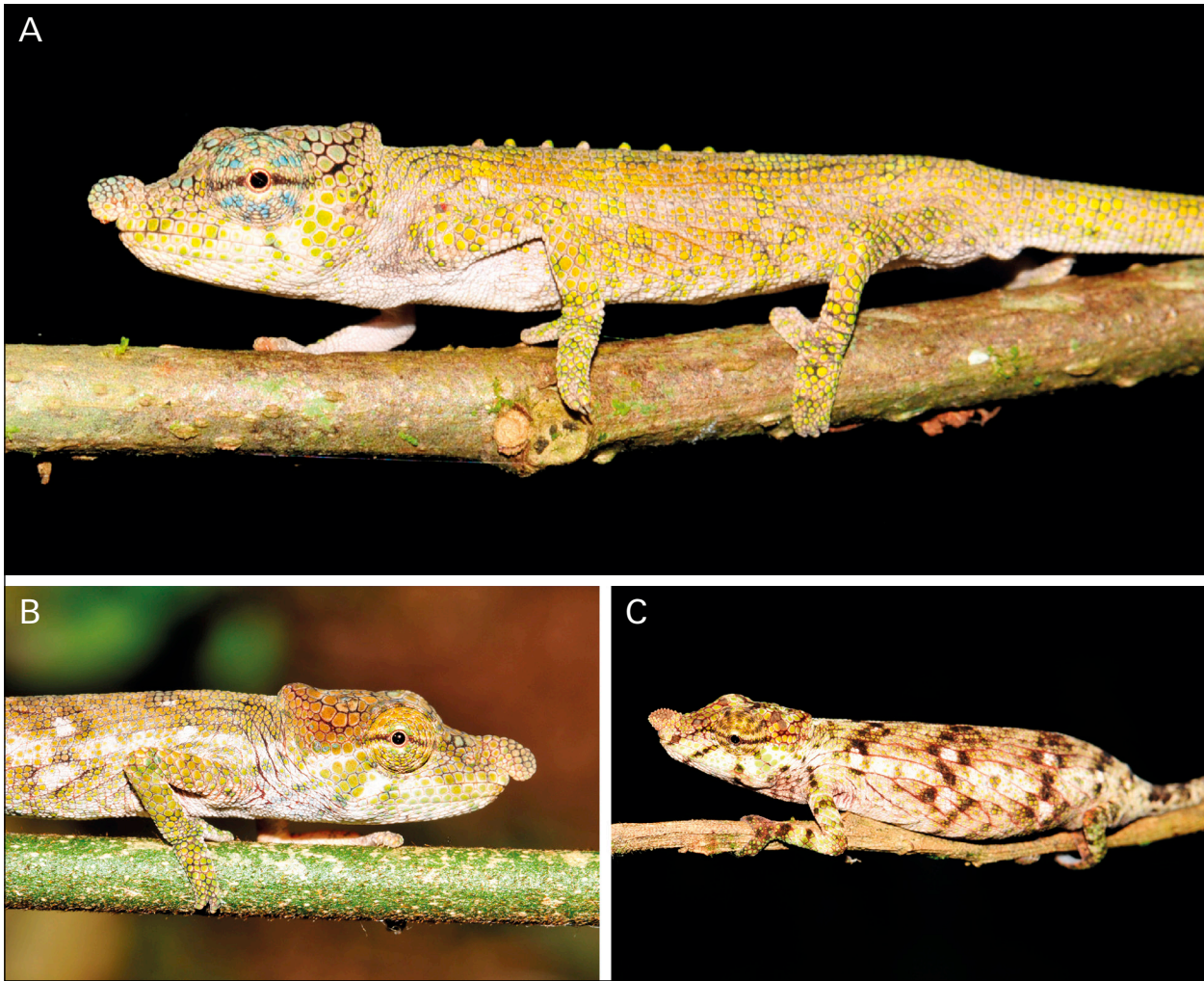


Fig. 8. *Calumma nasutum* (clade K) from Sorata, northern Madagascar. (A) juvenile male (FGCZ 3636, UADBA), slightly displaying; (B) adult female (not collected), relaxed; (C) adult female (ZSM 1699/2012) in stressed colouration.

length of the rostral appendage (2.6 vs 2.0–2.2 mm), the high casque (1.7–2.0 vs 1.5–1.7 mm), a similar number of infra- and supralabial scales (infralabials 13–15 vs 13–14, supralabials 14–15 vs 12–14), and similar skull morphology with the absence of a FF, parietal and squamosal connected, and similarly shaped parietals. Thus, the only available recently collected and sequenced male specimen from clade K (ZSM 924/2003) differs in some characters from the type series with a characteristically pointed casque, the presence of a parietal crest, presence of a dorsal crest (a variable character), and the absence of axillary pits. The specimens from Sorata form a subclade within K, of which only two adult females (ZSM 1699/2012 and ZSM 1700/2012) were available for detailed investigation; the specimens in the UADBA collection were not available for loan. These females show variation in morphology and osteology (see ‘Variation’) and also photographs from specimens in life, including a juvenile male, suggest some differentiation between the subclade from Sorata and that from Andasibe. Furthermore, there remains the possibility that clade K is not conspecific with *C. nasutum* and represents another new species. However, given the current state of knowledge,

the assignment to *C. nasutum* appears to be the most reasonable and parsimonious solution in order to avoid over-splitting and the unlikely assumption that the ‘true’ *C. nasutum* still awaits rediscovery. Further research and collection of more specimens may result in the need to re-evaluate this decision, but in the interest of resolving this complex, a pragmatic approach was required, especially since the attempts to obtain DNA from the lectotype (designated below) via a target enrichment approach were unsuccessful (N. STRAUBE, pers. comm.).

Lectotype designation: Due to the complicated taxonomy of the *C. nasutum* complex, there is an urgent need for a fixed, single specimen to represent *C. nasutum* and we therefore designate MNHN 6643C (1994/610), an adult male syntype, as the lectotype of *C. nasutum* (Fig. 4A). This specimen is the larger of the two males in the syntype series. The remaining syntypes, MNHN 6643, 6643A, and 6643B, become paralectotypes.

Referred material: ZSM 924/2003 (FG/MV 2002-0984), adult male, with completely everted hemipenes, collected in Andasibe (18.9333°S, 48.4167°E, 937 m a.s.l.), Toamasina Region, eastern Madagascar, on 18 February 2013 by G. Aprea; ZSM 454/2010

(FGZC 4506), adult male, collected in forest near Tarzanville (19.3244°S, 48.21988°E, 881 m a.s.l.), Alaotra-Mangoro Region, eastern Madagascar, on 13 April 2010 by F. Glaw, J. Köhler, P.-S. Gehring, K. Mebert, E. Rajeriarison; ZSM 256/2016 (FGZC 5283), near Maromizaha, Toamasina Region (18.9555°S, 48.4658°E, 927 m a.s.l.) on 02. August 2016 by F. Glaw, D. Prötzel, J. Forster, N. Raharinoro (not sequenced, assigned based on morphology only); ZSM 1699/2012 (FGZC 3711), adult female, collected on the Sorata massif at high elevation (about 13.68–13.69°S, 49.44°E, about 1060–1485 m a.s.l.), former Sava Region, northern Madagascar, on 29 November 2012 by F. Glaw, O. Hawlitschek, T. Rajoafiarison, A. Rakotoarison, F.M. Rasoavina, A. Razafimanantsoa; ZSM 1700/2012 (FGZC 3744) adult female; UADBA uncatalogued (FGZC 3740), adult male; UADBA uncatalogued (FGZC 3636), subadult male; UADBA uncatalogued (FGZC 3708), juvenile; all four collected on the Sorata massif (13.6772°S, 49.4413°E, 1394 m a.s.l.) on 30. November 2012 by F. Glaw, O. Hawlitschek, T. Rajoafiarison, A. Rakotoarison, F. M. Rasoavina, A. Razafimanantsoa.

Diagnosis (based on the type series and the referred material, see above; osteology based on micro-CT scans of the three males MNHN 6643C, MNHN 6643B, and ZSM 924/2003, and two females MNHN 6643 and ZSM 1699/2012): *Calumma nasutum* is characterised by (1) a medium size (male SVL 43.7–49.0 mm, female SVL 43.0–49.4 mm; male TL 89.0–100.8 mm, female 80.7–95.1 mm), (2) a medium sized (2.2–2.6 mm in males, 1.2–1.5 mm in females) and distally rounded rostral appendage, (3) rostral scale not integrated into the rostral appendage, (4–7) rostral, lateral, temporal (consisting of one tubercle), and cranial crests present, (8) parietal crest indistinct or present, (9) a distinctly raised casque in males with a height of 1.5–2.0 mm, (10) dorsal crest can be present in males, (11) 12–15 supralabial scales, (12) axillary pits generally present, (13) diameter of the largest scale in the temporal region of the head 0.8–1.6 mm, (14) no frontoparietal fenestra, (15) parietal and squamosal in contact, (16) parietal bone width at midpoint 9.8–17.9% of skull length; colour in life based on clade K: (17) a generally green to brown body colouration, (18) a typically olive green to brown nose in non-stressed colouration, (19) a green cheek colouration, (20) three to four diffuse dorsoventral blotches of variable colour on the body and a light lateral stripe, and (21) a brown stripe crossing the eye can occur.

Calumma nasutum can easily be distinguished from *C. vatsoa* by presence of a rostral appendage (vs absence); from *C. vohibola* by the rostral appendage length (1.2–2.6 mm vs 0.0–0.8 mm) and a high casque (0.7–2.0 mm vs 0.6 mm – re-measured, differing from GEHRING *et al.*, 2011); for diagnosis against *C. fallax*, see below. For diagnosis against the species described and revalidated herein, see their respective (re-)descriptions below.

Re-description of the lectotype (Fig. 4A): Adult male, with mouth slightly opened and tip of tongue between the jaws, in good state of preservation, hemipenes not everted. SVL 45.7 mm, tail length 55.5 mm, for other measurements, see Table 1; rostral ridges that give the snout a right angle, laterally compressed dermal rostral appendage of oval tubercle scales that projects straight forward over a length of 2.6 mm with a diameter of

2.2 mm, rounded distally and not including the rostral scale; 15 infralabial and 15 supralabial scales, all relatively small; supralabials with a serrated dorsal margin; indistinct lateral crest running horizontally; indistinct and short temporal crest consisting of one tubercle per side; indistinct cranial crest; no parietal crest; no occipital lobes; highly elevated (2.0 mm) and rounded casque; dorsal crest absent; no traces of gular or ventral crest. Body laterally compressed with fine homogeneous scalation with slightly larger scales on extremities and head region, largest scale in temporal region with diameter of 0.9 mm; deep axillary and less distinct inguinal pits.

Skull osteology of the lectotype (Fig. 1A): Skull length 12.3 mm; snout-casque length 15.6 mm; narrow paired nasals completely separated from each other by the anterior tip of frontal that meets the premaxilla; prefrontal fontanelle and naris separated by contact of prefrontal with maxilla; prominent prefrontal with laterally raised tubercles; frontal and parietal smooth with only a few tubercles; frontal with a width of 2.4 mm (19.5% of skull length) at border to prefrontal extending to 4.9 mm (39.8%) at border to postorbitofrontal; no frontoparietal fenestra; slightly curved parietal tapering strongly from a width of 5.0 mm (40.7%) at the border to postorbitofrontal to a width at midpoint of 1.2 mm (9.8%); posterodorsally directed parietal laterally in weak contact with the squamosals; squamosals thin without any tubercles. For further measurements, see Table 2.

Hemipenial morphology (based on clade K, Fig. 5D): medium sized calyces (hemipenial character A); two pairs of rotulae of different size, on sulcal side large with about 11 tips, on asulcal side small with about 5 tips (B); no papillary field (C); pair of short cornucula gemina (D), only visible when hemipenis fully everted.

Variation: For variation in measurements, see Table 1. The type series is morphologically highly homogeneous, and we therefore consider it likely that all of the type series belongs to a single species. However, the expression of the axillary pits varies between the specimens, possibly due to different fixation processes or the long period of storage in alcohol. The tail length of MNHN 6643B is exceptionally short in comparison to the other specimens. Specimens ZSM 924/2003 (genetic voucher) and ZSM 454/2010 differ from the other available material in a number of characters (see Assignment to genetic clade, above). Specimens from Sorata differ from the type series of *C. nasutum* and specimens from the Andasibe region by a distinct parietal crest over the whole length of the parietal bone (vs absence or short parietal crest), general absence of a cranial crest (vs generally present), the fine-scaled rostral appendage is oriented downwards vs of large tubercles and straight, low rounded casque (vs high and pointed). The species shows sexual dimorphism in tail length, which is longer in males than in females (RTaSV > 100% vs < 100%). The relative rostral appendage length does not differ.



Fig. 9. Distribution map of six species of the *Calumma nasutum* group in Madagascar. Localities based on collected specimens and/or DNA sequences of GEHRING *et al.* (2012) and new sequences shown in Fig. 2. Black stars within the symbols indicate type localities. Colours correspond to those used in Fig. 2.

Colouration in life (based on photographs of specimens assigned to clade K, Figs 7 & 8): Females generally more brown and less colourful than males; in both sexes olive green to brown body colouration, males can be yellowish when displaying, extremities and tail of same colour as the body; three to four diffuse lateral blotches of variable colour on the body and a light lateral stripe; throat and ventral region white or beige; rostral appendage typically olive green to brown; cheek region in olive to green colour; eyelids can be crossed by a brown stripe and with radiating turquoise stripes in displaying males.

Etymology: the Latin adjective *nasutum* meaning ‘big-nosed,’ in the neuter nominative singular; obviously in reference to the characteristic rostral appendage.

Distribution (Fig. 9): *Calumma nasutum*, as redefined here, is known from eastern Madagascar between Anosibe An’ala (19.3244°S, 48.2199°E) and Andasibe in the central east to Sorata, more than 600 km further north (see coordinates above), from an elevation of 880–1400 m a.s.l.

Identity, revalidation, and re-description of *Calumma radamanus* (Mertens, 1933)

ZOOBANK urn:lsid:zoobank.org:act:338C6481-C673-49DC-A8C2-156F02C1F5E9

Chamaeleo radamanus Mertens, 1933; synonymy fide ANGEL (1942) with *Chamaeleo nasutus* Duméril & Bibron, 1836; this synonymy was accepted by MERTENS (1966).

Taxonomic notes and justification of revalidation:

Chamaeleo radamanus was described by MERTENS (1933) on the basis of 17 adult and three subadult specimens. Measurements, however, were only provided from two adult males and one female. These three individuals are still present in the collection of the Senckenberg Museum of Frankfurt (SMF) and were analysed here. Several of the paratypes were exchanged with other museums and their whereabouts remain unknown; we were able to trace only three of these specimens, which are housed in the Naturhistorisches Museum Wien (NMW), see below. *Chamaeleo radamanus* was synonymized with *Ch. nasutum* by ANGEL (1942) based on the establishment of the former based on variable characters that are sexually dimorphic – we note that Angel himself apparently did not examine any of the type material of *C. radamanus*, but based this assessment on the photos presented by MERTENS (1933). As is explained in greater detail in the re-description below, the members of this species differ from *C. nasutum sensu stricto* (as redefined here) in several characteristics, such as the rostral scale integration into the rostral appendage (integrated vs not integrated), direction of the rostral appendage (down vs up or straight), shorter rostral appendage in males (2.9–3.6% of SVL vs 4.5–5.3% of SVL) squamosal shape (short posterior process of squamosal widely separated from parietal vs meeting the parietal), and frontal width (very broad vs narrow at midpoint). Given these differences, we consider the morphology of *C. radamanus* to be sufficiently different from *C. nasutum* as to warrant treatment as a separate species. Additionally, the morphology of the holotype closely matches specimens of clade GII (Figs 2, 6B, 10); a specimen of that clade has been depicted before in GEHRING *et al.* (2011) as *Calumma* sp. aff. *nasutum*, Tampolo. We therefore here attribute *C. radamanus* to clade GII, resurrect the species from synonymy, and re-describe it here.

Holotype: SMF 22132, adult male, collected in 1931 by Hans Bluntschli in Col Pierre Radama 1000 m a.s.l. (= Ambatondradama or Ambatoledama, 35–40 km northeast of Maroantsetra, N.E. Madagascar according to VIETTE (1991); coordinates approximately: 15.29°S, 50.00°E, ca. 547 m a.s.l.; see also GEHRING *et al.* (2011).

Paratypes: At least the following five specimens: SMF 26394 (female), SMF 26367 (subadult male), NMW 15999:1 (male with everted hemipenes), NMW 15999:2 (female) and NMW 15999:3 (female), all with presumably the same collection data as the holotype. The current whereabouts and institutional numbers of the remaining 14 type specimens are unknown (GEHRING *et al.*, 2011).

Assignment to genetic clade (based on a comparison of the holotype with all specimens from clade G, Fig. 2): On the basis of the short, downward oriented rostral appendage, which has the rostral scale integrated into it and the relatively short tail length, and on the basis of its skull osteology, in particular the broad frontal and parietal

bones, the relatively short postparietal process, the short posterior process of the squamosal that does not contact the parietal, and the broad and crenate lateral margins of the prefrontals, *C. radamanus* belongs to clade G. This clade is divided into five subclades genetically that are morphologically quite strongly conserved, see Fig. 2.

To maximise the precision of our definition, we tentatively assign the holotype to subclade GII (based on the holotype and specimens of clade GII=referred material, for osteology SMF 22132, ZSM 619/2009, ZSM 475/2010, all three males): the type series of *Calumma radamanus* and clade GII have an overlapping size of, for example, the rostral appendage in males of 1.6 vs 1.4–1.7 mm, a short tail (96% of SVL vs 90–99% of SVL), and the most similar osteology (e.g. relative parietal width 19.3% vs 16.1–22.4%). This clade also makes sense biogeographically, being the nearest of the members of the G clade to the type locality of the species.

We here delimit *Calumma radamanus* (n=10) from specimens of clade GI (Nosy Be and Nosy Komba, Figs 2 & 9, n=4), GIII (Vohimana, Vohidrazana, Sahafina, Moramanga, n=5), GIV (Marojejy, n=6), and GV (Sorata, Fanambana, n=15), with the aid osteological data (for *C. radamanus* ZSM 619/2009 and ZSM 475/2010, both males) based on the following specimens: ZSM 88/2015, female of clade GI, ZSM 145/2016 and ZSM 451/2016, both males of clade GIII, ZSM 441/2005, male of clade GIV, and ZSM 1694/2012 and ZSM 1691/2012, both males of clade GV. The subclade GII differs from GIII by a shorter rostral appendage (in males 1.4–1.7 mm vs 3.0–3.3 mm, in females 0.2–1.6 mm vs 1.6–2.5 mm), dorsal crest occasionally present in males and absent in females vs present in males and generally present in females, and a relatively wider frontal (RFPo 38.1–42.2% vs 36.2–36.3%); from clade GIV by a shorter rostral appendage (in males 1.4–1.7 mm vs 3.0–3.1 mm, in females 0.2–1.6 mm vs 1.7–2.4 mm), shorter relative parietal length (RPL 37.3–40.5% vs 44.2%), and shorter relative snout-casque length (RSCL 114.4–119.0% vs 123.3%); from clade GV by shorter rostral appendage in males (1.4–1.7 mm vs 1.8–3.4 mm), temporal crest usually present vs absent, shorter relative parietal length (RPL 37.3–40.5% vs 40.5–47.0%), and shorter relative snout-casque length (RSCL 114.4–119.0% vs 121.4–126.5%).

In order to avoid over-splitting in the absence of adequate data, and despite our relatively large sample size, we here refrain from a taxonomic assignment of the remaining genetic lineages within clade G to any taxon, and instead refer these to unconfirmed candidate species within the *C. radamanus* species complex, that will certainly need a future taxonomic revision with a considerably bigger dataset.

Referred material (specimens of the clade GII): ZSM 443/2005 (ZCMV 2169), adult male, collected on Nosy Mangabe (about 15.50°S, 49.76°E, about 50–100 m a.s.l.), Analanjirifo Region, northeastern Madagascar, on 22 February 2005 by F. Glaw, M. Vences, R.D. Randrianiana; ZSM 619/2009 (ZCMV 11293), adult

male, collected on the Makira Plateau (about 15.44°S, 49.12°E, about 1000 m a.s.l.), Analanjirifo Region, northeastern Madagascar, on 22–25 June 2009 by M. Vences, D.R. Vieites, F.M. Ratsavina, R.D. Randrianiaina, E. Rajeriarison, T. Rajofiarison, J. Patton; ZSM 475/2010 (FGZC 4313), adult male, collected in Ambodivoahangy (15.2899°S, 49.6202°E, about 100 m a.s.l.), Analanjirifo Region, northeastern Madagascar, on 03 April 2010 by F. Glaw, J. Köhler, P.-S. Gehring, M. Pabijan, F.M. Ratsavina; ZSM 152/2016 (FGZC 5152), adult female, collected near Analalava (17.7070°S, 49.4598°E, about 30 m a.s.l.), Analanjirifo Region, northeastern Madagascar, on 01 January 2016 by F. Glaw, D. Prötzel, L. Randriamanana; ZSM 646/2009 (ZCMV 8957), juvenile female, collected in Tampolo forest (17.2886°S, 49.4115°E, 7 m a.s.l.), Analanjirifo Region, northeastern Madagascar, on 26 April 2009 by P.-S. Gehring, F.M. Ratsavina, E. Rajeriarison; ZSM 259/2016 (FGZC 5433), adult female, collected in Masoala near Eco-Lodge Chez Arol (15.7121°S, 49.9639°E, 21 m a.s.l.), Analanjirifo Region, northeastern Madagascar, on 10 August 2016; ZSM 260/2016 (FGZC 5453), juvenile male, collected in Masoala near Eco-Lodge Chez Arol (15.7247°S, 49.9599°E, 14 m a.s.l.) on 14 August 2016, both by F. Glaw, D. Prötzel, J. Forster, K. Glaw, T. Glaw.

Diagnosis (based on the type series and the referred material, see above; osteology based on SMF 22132, ZSM 619/2009, and ZSM 475/2010, all three males): *Calumma radamanus* is characterised by (1) a medium size (male SVL 42.6–49.2 mm, female SVL 43.0–49.2 mm; male TL 84.9–93.5 mm, female TL 77.0–92.9 mm), tail length shorter than body length, (2) a short (1.4–1.7 mm in males, 0.2–1.6 mm in females) and distally rounded, downward oriented rostral appendage, (3) rostral scale generally integrated into the rostral appendage, (4) rostral crest present, (5) lateral crests present, (6) temporal crest generally present, (7) cranial crest present, (8) parietal crest absent, (9) an indistinctly raised casque in males with a height of 0.8–1.5 mm, (10) a dorsal crest of 6–8 spines sometimes present in males, absent in females, (11) 11–15 supralabial scales with a serrated upper margin, (12) general absence of axillary pits, (13) diameter of the largest scale in the temporal region of the head 0.6–0.9 mm, (14) no frontoparietal fenestra in the skull, (15) posterior process of squamosal widely separated from parietal, (16) parietal bone width at midpoint 16.1–22.4% of skull length, (17) a generally greenish body colouration, (18) a typically turquoise nose in non-stressed colouration, (19) a turquoise cheek colouration, (20) three royal blue dorsoventral blotches on the body and a white lateral stripe, and (21) a brown to black stripe running from rostral appendage across the eye to the casque.

Calumma radamanus can easily be distinguished from all species of the *C. boettgeri* complex (see above) by the absence of occipital lobes; from *C. gallus* by different length, shape and colour of its rostral appendage (see above); from *C. vatosoa* by presence of a rostral appendage (vs absence); from *C. vohibola* by generally longer relative rostral appendage length (RRS 0.5–3.6% vs 0.1–1.4%), rostral scale generally integrated into rostral appendage (vs not integrated), squamosal and parietal not in contact (vs in contact), wider frontal bone, crenate prefrontals (vs smooth), greenish body colouration (vs greyish to brownish), presence of large blue

lateral blotches (vs absence); from *C. nasutum* as redefined herein generally by rostral scale integrated into the rostral appendage (vs not integrated), shorter rostral appendage in males (2.9–3.2% of SVL vs 4.5–5.3%), male casque lower (0.8–1.5 mm vs 1.5–2.0 mm), occasional presence of dorsal crest consisting of spines (vs generally absence or consisting of cones if present), squamosal and parietal not in contact (vs in contact); for diagnosis against *C. fallax*, see below. For diagnosis against the species described herein, see their respective descriptions below.

Description of the holotype (Fig. 4): Adult male, with mouth closed, in good state of preservation except for the ventrally sliced body, hemipenes not everted. SVL 44.5 mm, tail length 42.6 mm, for other measurements, see suppl. Table 1; rostral ridges that give the snout a right angle, laterally compressed dermal rostral appendage of oval tubercle scales that projects downwards over a length of 1.6 mm with a diameter of 1.8 mm and includes the rostral scale; 11 infralabial and 13 supralabial scales, all rather small; supralabials with a serrated dorsal margin; distinct lateral crest running horizontally; temporal crest consisting of one tubercle per side; distinct cranial crest; no parietal crest; no occipital lobes; medium sized (1.5 mm height) and rounded casque; no trace of a dorsal or gular or ventral crest. Body laterally compressed with fine homogeneous scalation and larger scales on extremities and head region, largest scale in temporal region with diameter of 0.8 mm and in cheek region of 1.1 mm; no axillary or inguinal pits.

Skull osteology of the holotype (Fig. 1D): Skull length 11.9 mm; snout-casque length 14.1 mm; narrow paired nasals completely separated from each other by the anterior tip of frontal that meets the premaxilla; prefrontal fontanelle and naris fused; prominent prefrontal with laterally raised tubercles exceeding more than the half of the prefrontal fontanelle; frontal and parietal smooth without any tubercles; frontal with a width of 3.4 mm (28.6% of skull length) at border to prefrontal extending to 4.8 mm (40.3%) at border to postorbitofrontal; no frontoparietal fenestra; triangular parietal with a width of 4.0 mm (33.6%) at the border to postorbitofrontal and a width at midpoint of 2.3 mm (19.3%) tapering continuously posterodorsally; short squamosals far from meeting the parietal. For further measurements, see Table 2.

Hemipenial morphology, based on ZSM 443/2005 (Fig. 5B): Large calyces (hemipenial character A); two pairs of small rotulae on apex of about the same size (B), finely denticulated with about 12–15 tips each; papillary field of small, unpaired papillae (C); cornucula gemina absent (D).

Variation: The specimens SMF 22132 and SMF 26394 show narrow and irregularly shaped openings in the skull roof. We suggest that these are associated with the



Fig. 10. *Calumma radamanus* in life. (A) adult male (not collected) from Tampolo, eastern Madagascar, in relaxed state, photo: P.-S. Gehring; (B, C) juvenile male (ZSM 260/2016) from Masoala, relaxed; (D) adult female from Masoala (not collected), relaxed.

juvenile state of these specimens, and adult specimens indicate that a frontoparietal fenestra does not persist into adulthood. For variation in measurements, see Table 1. Sexual dimorphism: Males are slightly larger than females and they have a relatively longer tail (RTaSV 90–100% vs 79–89%). However, the relative length of the rostral appendage does not differ. A dorsal crest occurs only in males, if present at all.

Colouration in life (Fig. 10): No strong dichromatism between sexes; green to beige body colouration, extremities and tail of same colour as the body; a beige-white (can be inverted to black) lateral stripe may occur from the casque to the hip that crosses the three lateral blotches of distinct blue or violet colour; throat and ventral region white or beige; rostral appendage turquoise or blue; in males, a brown lateral stripe from nostrils, crossing

the eyes and fading towards the tip of the casque; cheek region highlighted in turquoise or bright green colour; males appear to be more brightly coloured.

Etymology: Radamanus means ‘from Radama’ in Latin (-anus declension meaning ‘of’ or ‘pertaining to’), and clearly refers to the origin of specimens from Col Pierre Radama. However, it is not clear from the word ‘radamanus’ nor from the original description whether this is to be treated as a substantive noun or an adjective. Thus article 31.2.2 of The International Code of Zoological Nomenclature (INTERNATIONAL COMMISSION ON ZOOLOGICAL NOMENCLATURE 1999) has to be applied: ‘Where the author of a species-group name did not indicate whether he or she regarded it as a noun or as an adjective, and where it may be regarded as either and the evidence of usage is not decisive, it is to be treated as a noun in ap-

position to the name of its genus.' Given that the taxon *Chamaeleo radamanus* disappeared soon after its description into the synonymy of *C. nasutum*, there was no decisive usage of this name (see above). Therefore, the name is to be considered an invariable noun in apposition, and its declension is not changed.

Distribution (Fig. 9): *Calumma radamanus* sensu stricto as redefined here, is known from eastern Madagascar between Tampolo and the type locality Ambatond'Radama about 250 km further north (for coordinates, see above), from an elevation of about 7–500 m a.s.l. (see Fig. 9). For the distribution of the *C. radamanus* complex, see Fig. 9. Specimens from Montagne d'Ambre were not analysed here, but probably also belong to the *C. radamanus* complex, based on overall appearance.

Description of *Calumma emelinae* sp. nov.

ZOOBANK urn:lsid:zoobank.org:act:EE10A0D2-832F-4CBE-81E0-10E6CADB4A76

Remark: This new species refers to clade B of Fig. 2 and GEHRING *et al.* (2012).

Holotype: ZSM 618/2009 (ZCMV 11292), adult male with completely everted hemipenes, right hemipenis cut off for micro-CT scanning, collected in the Makira plateau, Angozongahy or Ampofoko (about 15.44°S, 49.12°E, 1000 m a.s.l.), Analanjirofo Region, northeastern Madagascar, on 22–25 June 2009 by M. Vences, D.R. Vieites, F.M. Ratoavina, R.D. Randrianiaina, E. Rajeriarison, T. Rajofiarison, J. Patton.

Paratypes: ZSM 660/2014 (DRV 5899), ZSM 663/2014 (DRV 5898), both adult males, collected in Angozongahy, western side of Makira plateau camp 1 (15.4370°S, 49.1186°E, 1009 m a.s.l.), Analanjirofo Region, northeastern Madagascar, on 26 June 2009 by M. Vences, D.R. Vieites, F.M. Ratoavina, R.D. Randrianiaina, E. Rajeriarison, T. Rajofiarison, J. Patton; ZSM 553/2001 (MV 2001-239), adult female, collected in Andasibe (about 18.93°S, 48.42°E, 900 m a.s.l.), Alaotra-Mangoro Region, eastern Madagascar, on 16–18 February 2001 by M. Vences, D.R. Vieites; ZSM 135/2005 (FGZC 2692) and ZSM 136/2005 (FGZC 2693), both adult females and collected in Vohidrazana (about 18.95°S, 48.50°E, 700–800 m a.s.l.), Alaotra-Mangoro Region, eastern Madagascar, on 09 February 2005 by F. Glaw, R.D. Randrianiaina, R. Dolch; ZSM 661/2014 (DRV 5677) and ZSM 662/2014 (DRV 5708), both adult females, collected in Mahasoa campsite near Ambodisakoa village (NE Vohimena, NE Lake Alaotra, 17.2977°S, 48.7019°E, 1032 m a.s.l.), Alaotra-Mangoro Region, eastern Madagascar, on 13–15 February 2008 by D.R. Vieites, J. Patton, P. Bora, M. Vences; ZSM 148/2016 (FGZC 5236), adult female, collected east of Moramanga in 'Julia Forest' (18.9511°S, 48.2719°E, 941 m a.s.l.) on 6 January 2015; ZSM 147/2016 (FGZC 5175), adult female collected south of Moramanga (19.0192°S, 48.2341°E, 903 m a.s.l.), Alaotra-Mangoro Region, eastern Madagascar, on 4 January 2016, both by F. Glaw, D. Prötzel, L. Randriamanana.

Diagnosis (based on the type series; osteology based on micro-CT scan of ZSM 618/2009, male): *Calumma emelinae* sp. nov. is characterised by (1) a medium size (male SVL 46.6–48.7 mm, female SVL 40.1–49.1 mm; male TL 93.6–103.2 mm, female TL 82.7–95.8 mm), (2) a medium (2.3–2.9 mm in males 1.5–1.8 mm in females) and distally rounded rostral appendage, (3) rostral

scale not integrated into the rostral appendage, (4) rostral crest present, (5) lateral crest present, (6) temporal crest present, (7) cranial crest variable, (8) parietal crest usually absent, (9) casque low in males with a height of 0.5–1.1 mm, (10) a dorsal crest of 7–10 spines in males, absent in females, (11) 12–16 supralabial scales with a mostly straight upper margin, serrated anteriorly, (12) absence of axillary pits, (13) diameter of the largest scale in the temporal region of the head 0.6–1.0 mm, (14) no frontoparietal fenestra, (15) parietal and squamosal in contact, (16) parietal bone width at midpoint 16.2% of skull length (n=1), (17) a generally greyish to greenish body colouration, (18) rostral appendage colour generally unremarkable, (19) a green cheek colouration, (20) suggestions of two weak bluish lateral blotches, and (21) no strong eye colouration.

Calumma emelinae sp. nov. can easily be distinguished from all species of the *C. boettgeri* complex (see above) by the absence of occipital lobes; from *C. gallus* by different length, shape and colour of its rostral appendage (see above); from *C. vatosoa* by presence of a rostral appendage (vs absence); from *C. vohibola* by generally longer relative rostral appendage length (RRS 3.1–6.1% vs 0.1–1.4%), dorsal crest always present in males (vs generally absent), and pointed tip of postparietal process (vs relatively broad), and crenate prefrontal (vs smooth); from *C. nasutum* as redefined herein by a lower casque in males (0.5–1.1 mm vs 1.5–2.0 mm), dorsal crest present in males consisting of spines (vs general absence or consisting of cones if present), and scales more homogeneous (largest temporal scale in males 0.7 mm vs 0.9–1.6 mm); from *C. radamanus* by relatively longer tail in males (longer than SVL vs shorter), longer rostral appendage in males (RRS 4.7–6.1% vs 2.9–3.6%), rostral scale not integrated into rostral appendage (vs integrated), supralabials with a largely straight upper margin (vs serrated), and parietal and squamosal in contact (vs widely separated); for diagnosis against *C. fallax*, see below. For diagnosis against the other species described herein, see their respective descriptions below.

Description of the holotype (Fig. 4C): Adult male, with mouth closed, in good state of preservation, both hemipenes fully everted; SVL 47.9 mm, tail length 50.7 mm, for other measurements, see suppl. Table 1; rostral ridges that give the snout a right angle; laterally flattened and distally rounded rostral appendage of small tubercle scales that projects straight forward over a length of 2.9 mm with a diameter of 2.4 mm not including the rostral scale; 14 infralabial and 15 supralabial scales, both rather small; supralabials with a straight upper margin; distinct lateral crest running horizontally; no temporal or cranial crest; low parietal crest; no occipital lobes; very low casque of 0.5 mm height; dorsal crest consisting of 10 spines; no gular or ventral crest. Body laterally compressed with fine homogeneous scalation and slightly larger scales on extremities and head region, largest scale in temporal region with diameter of 0.7 mm and in cheek region of 0.9 mm; no axillary or inguinal pits.

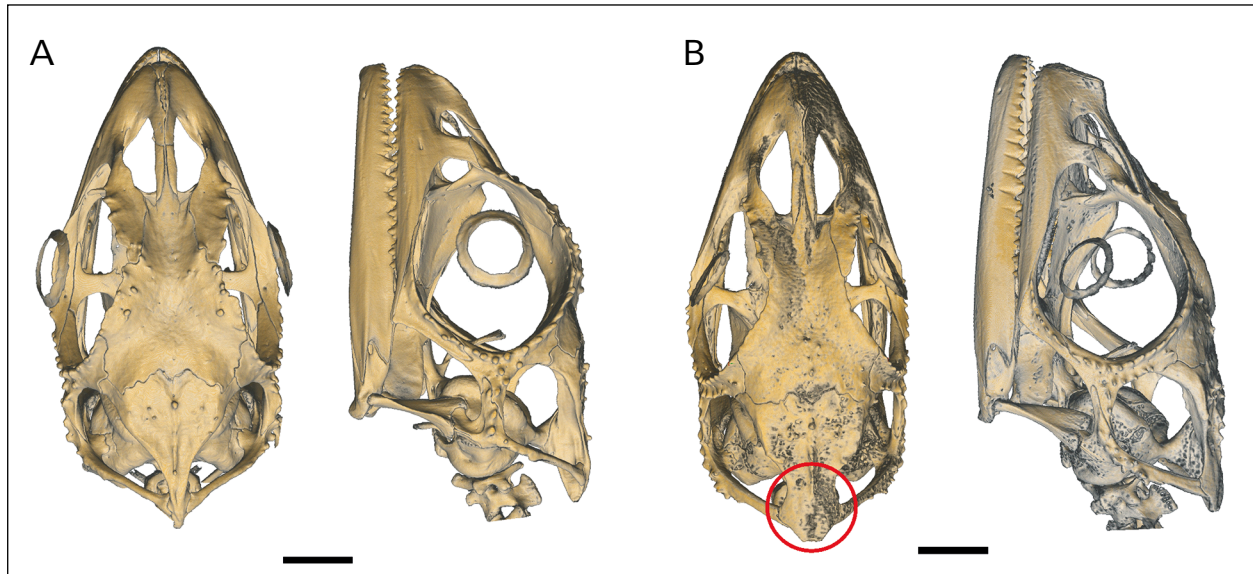


Fig. 11. Micro-computed tomography scans of the skulls of holotypes of species with a closed skull roof in dorsal and lateral view. (A) *C. emelinae* sp. nov. (ZSM 618/2009), male holotype; (B) *C. tjiasmantoi* sp. nov. (ZSM 735/2003), female holotype. Diagnostic characters are encircled in red. Scale bars: 2.0 mm.

Skull osteology of the holotype (Fig. 11A): Skull length 11.7 mm; snout-casque length 13.8 mm; narrow paired nasals still slightly connected at anterior end; anterior tip of frontal extending to about the middle of the prefrontal fontanelle, which is fused with the naris; prominent and broad prefrontal with laterally raised tubercles; frontal and parietal covered with a few tubercles; frontal with a width at border to prefrontal of 3.0 mm (25.6% of skull length) extending to 4.4 mm (37.6%) at border to postorbitofrontal; no frontoparietal fenestra; narrow parietal with a width at the border to postorbitofrontal of 4.2 mm (35.9%) and a width at midpoint of 1.9 mm (16.2%) tapering strongly posterodorsally; parietal laterally in strong contact with the squamosals; squamosals relatively thick and covered with several tubercles. For further measurements, see Table 2.

Hemipenial morphology, based on ZSM 618/2009 (Fig. 5C), ZSM 660/2014 and ZSM 663/2014: medium sized calyces (hemipenial character A); two pairs of small rotulae on apex of about the same size (B), roughly denticulated with about 9–12 tips each; papillary field of small, unpaired papillae (C); pair of short cornucula gemina (D), only visible when hemipenis fully everted.

Variation: For variation in measurements, see Table 1. Sexual dimorphism: Males are usually larger than females (mean TL of 98.5 mm vs 88.3 mm). Tail length is generally longer in males than in females (RTaSV > 100% vs < 100%), as well as the length of the rostral appendage (> 2.0 mm vs < 2.0 mm).

Colouration in life (Fig. 12): Both sexes with an indistinct brown to beige body colouration, extremities and tail of same colour as the body; three diffuse/scattered brown dorsoventral blotches can occur on the body;

males can show a beige lateral stripe; throat and ventral region beige; rostral appendage not accentuated; cheek region can be light green; eyelids crossed by a brown stripe and occasionally with radiating dark green stripes in both sexes.

Etymology: The specific epithet is named after Emelina Widjojo, the mother of Wewin Tjiasmanto, in recognition of her support for taxonomic research and nature conservation projects in Madagascar through the BIOPAT initiative (<http://biopat.de/en/>).

Distribution (Fig. 9): *Calumma emelinae* sp. nov. is known in eastern Madagascar from Anosibe An'Ala to Angozongahy (Makira) about 500 km further north (for coordinates, see above), from an elevation of 750–1030 m a.s.l.

Description of *Calumma tjiasmantoi* sp. nov.

ZOOBANK urn:lsid:zoobank.org:act:65471E38-67B4-4BC0-9CC9-402B8214A7A8

Remark: This new species refers to clade J of Fig. 2 and GEHRING *et al.* (2012). Due to uncertainties about the collection data of the only male specimen we designate a well-documented female as the holotype.

Holotype: ZSM 735/2003 (FG/MV 2002-497), adult female collected in Ranomafana National Park (21.2639°S, 47.4194°E, 983 m a.s.l.), Vatovavy-Fitovinany Region, eastern Madagascar, on 23 January 2003 by F. Glaw, M. Puente, L. Raharivololoniaina, M. Thomas, D.R. Vieites.

Paratypes: ZSM 312/2006 (ZCMV 2896), adult male, and UADBA uncatalogued (ZCMV 2895), female, both collected in Ranomafana, probably Ambatolahy (21.2439°S, 47.4262°E, 919 m a.s.l.) on 21 February 2006 by M. Vences; ZSM 723/2003 (FG/MV 2002-



Fig. 12. *Calumma emelinae* sp. nov. in life. (A) adult male (not collected) from the type locality in Makira in stress colouration; (B) sub-adult male (not collected) from Mahasoa, in relaxed state; (C) adult female (not collected) from Makira, slightly stressed; (D) adult female (FGZC 5273, UADBA uncatalogued) from east of Moramanga ('Julia Forest') in relaxed state; (E) adult female (uncollected) from same location as (D), relaxed.

0396) and ZSM 736/2003 (FG/MV 2002-0498), both adult females, same collection data as holotype; ZSM 380/2016 (ZCMV 14835), adult female, collected in Sampanandrano (24.1399°S, 47.0742°E, 539 m a.s.l.), Atsimo-Antsinanana Region, southeastern Madagascar, on 16 December 2016 by A. Rakotoarison, E. Rajeriarison, J.W. Ranaivosolo.

Diagnosis (based on the type series, osteology based on micro-CT scan of ZSM 735/2003, female): *Calumma tjiasmantoi* sp. nov. is characterised by (1) a small size

(male SVL 43.9–46.8 mm, female TL 84.1–94.8 mm); (2) a medium sized (1.1–2.1 mm) and distally rounded rostral appendage, (3) rostral scale not integrated into the rostral appendage, (4–8) rostral, lateral, temporal, cranial, and parietal crests present, (9) casque medium sized in males (1.3 mm), (10) a dorsal crest of 7–9 spines can be present in males (based also on photographs), absent in females, (11) 15–17 supralabial scales with a mostly straight upper margin, (12) general absence of axillary

pits, (13) diameter of the largest scale in the temporal region of the head 0.6–0.8 mm, (14) frontoparietal fenestra absent, (15) parietal and squamosal in contact, (16) parietal bone width at midpoint 16.1% of skull length ($n=1$) with a characteristic broad tip to the postparietal process, (17) bright green or yellowish body colouration in males, females generally browner and less conspicuous, (18) rostral appendage colour generally inconspicuous, (19) cheek colouration greenish to turquoise, (20) five characteristic dorsoventral stripes of blue or brown colour, and (21) a diffuse brown stripe crossing the eye.

Calumma tjiasmantoi sp. nov. can easily be distinguished from all species of the *C. boettgeri* complex (see above) by the absence of occipital lobes; from *C. galus* by different length, shape and colour of its rostral appendage (see above); from *C. vatosoa* by presence of a rostral appendage (vs absence); from *C. vohibola* by longer rostral appendage in females (RRS 2.4–4.6% vs 0.2–0.7%), parietal crest present (vs absent), smaller temporal scale (0.6–0.8 mm vs 1.0 mm); from *C. nasutum* as redefined herein by the higher number of supralabials (15–17 vs 12–15), a shorter rostral appendage (4.3% of SVL vs 4.5–5.3% of SVL), a shorter parietal (36.3% of skull length vs 41.0–44.3%), broad postparietal process (vs narrow); from *C. radamanus* by a relatively longer tail in females (RTaSV 92–95% vs 79–89%), rostral scale not integrated in rostral appendage (vs generally integrated), parietal crest present (vs absent), more supralabials (15–17 vs 11–15) with a generally straight upper margin (vs serrated), parietal and squamosal in contact (vs widely separated); from *C. emelinae* sp. nov. by presence of parietal crest (vs usually absent), absence of lateral white stripe, and broader postparietal process; for diagnosis against *C. fallax*, see below. For diagnosis against the other species described herein, see its description below.

Description of the holotype (Fig. 4D): Adult female, with mouth closed, in good state of preservation except for a ventrally sliced body, with four eggs still fixed in the oviduct; SVL 45.5 mm, tail length 42.5 mm, for other measurements, see suppl. Table 1; bulging rostral ridges; laterally flattened and distally rounded rostral appendage of tubercle scales that projects straight forward over a length of 1.7 mm with a diameter of 1.4 mm not including the rostral scale; 15 infralabial and 15 supralabial scales, all rather small; most of the supralabials with a straight upper margin, only anterior scales serrated; distinct lateral crest running horizontally; temporal crest consisting of two tubercles; short cranial crest; short parietal crest; no occipital lobes; medium sized casque of 1.1 mm height; no dorsal, gular or ventral crest. Body laterally compressed with fine homogeneous scalation and only slightly larger scales on extremities and head region, largest scale in temporal region with diameter of 0.6 mm and in cheek region of 0.6 mm; no axillary or inguinal pits.

Skull osteology of the holotype (Fig. 11B): Skull length 12.4 mm; snout-casque length 14.4 mm; narrow paired

nasals anteriorly still in contact; anterior tip of frontal not exceeding the middle of the prefrontal fontanelle, which is fused with the naris; prominent and broad prefrontal with laterally raised tubercles; frontal and parietal smooth with only a few tubercles; frontal with a width of 2.4 mm (19.4% of skull length) at border to prefrontal extending to 4.3 mm (34.7%) at border to postorbitofrontal; no frontoparietal fenestra; broad parietal with distinct parietal crest tapering slightly from a width of 4.3 mm (34.7%) at the border to postorbitofrontal to a width at midpoint of 2.0 mm (16.1%); the posterodorsally broadened end is in strong contact with the squamosals; squamosals broad with several tubercles. For further measurements, see Table 2.

Hemipenial morphology, based on ZSM 312/2006 (no micro-CT scan available): medium sized calyces (hemipenial character A); two pairs of small rotulae on apex of about the same size (B), finely denticulated with about 7–9 tips each; papillary field of small, unpaired papillae (C); pair of medium sized cornucula gemina (D), only visible when hemipenis fully everted.

Variation: For variation in measurements, see Table 1. For variation in colouration in life, see Fig. 13. The female ZSM 134/2005 (FGZC 2508) from Andohahela at high elevation (1548 m a.s.l.) belongs genetically to clade J but shows substantial morphological differences so that we do not designate it as a paratype. Aside from a larger total length (97.0 mm), a longer rostral appendage (2.6 mm), and a low number of supralabials (12) it also has a unique skull morphology with a FF. This correlates well with a previous study where only high elevation species tend to have a FF (PRÖTZEL *et al.*, 2018b) but does not fit in the general pattern of *C. tjiasmantoi* sp. nov. Further studies are necessary to clarify this apparent contradiction in our dataset and potential taxonomic conclusions. Sexual dimorphism: Body size (SVL and TL) is slightly larger in males than females, tail length is longer in males than in females (RTaSV 103% vs 92–95%), and a dorsal crest is only present in males.

Colouration in life: Strong sexual dichromatism with males of bright green or yellowish body colouration and turquoise extremities and females generally browner and less conspicuous. In both sexes five diffuse dorsoventral stripes on the body – in males of blue colour with light spots, in females of brown colour; no lateral stripe across the body; tail annulated, continuing the blotches from the body; throat and ventral region can be beige or of same colour as the body; indistinct rostral appendage not accentuated from the head; cheek region turquoise in males; a diffuse brown stripe may cross the eye.

Etymology: The specific epithet is a patronym honouring Wewin Tjiasmanto in recognition of his support for taxonomic research and nature conservation projects in Madagascar through the BIOPAT initiative (<http://biopat.de/en>).

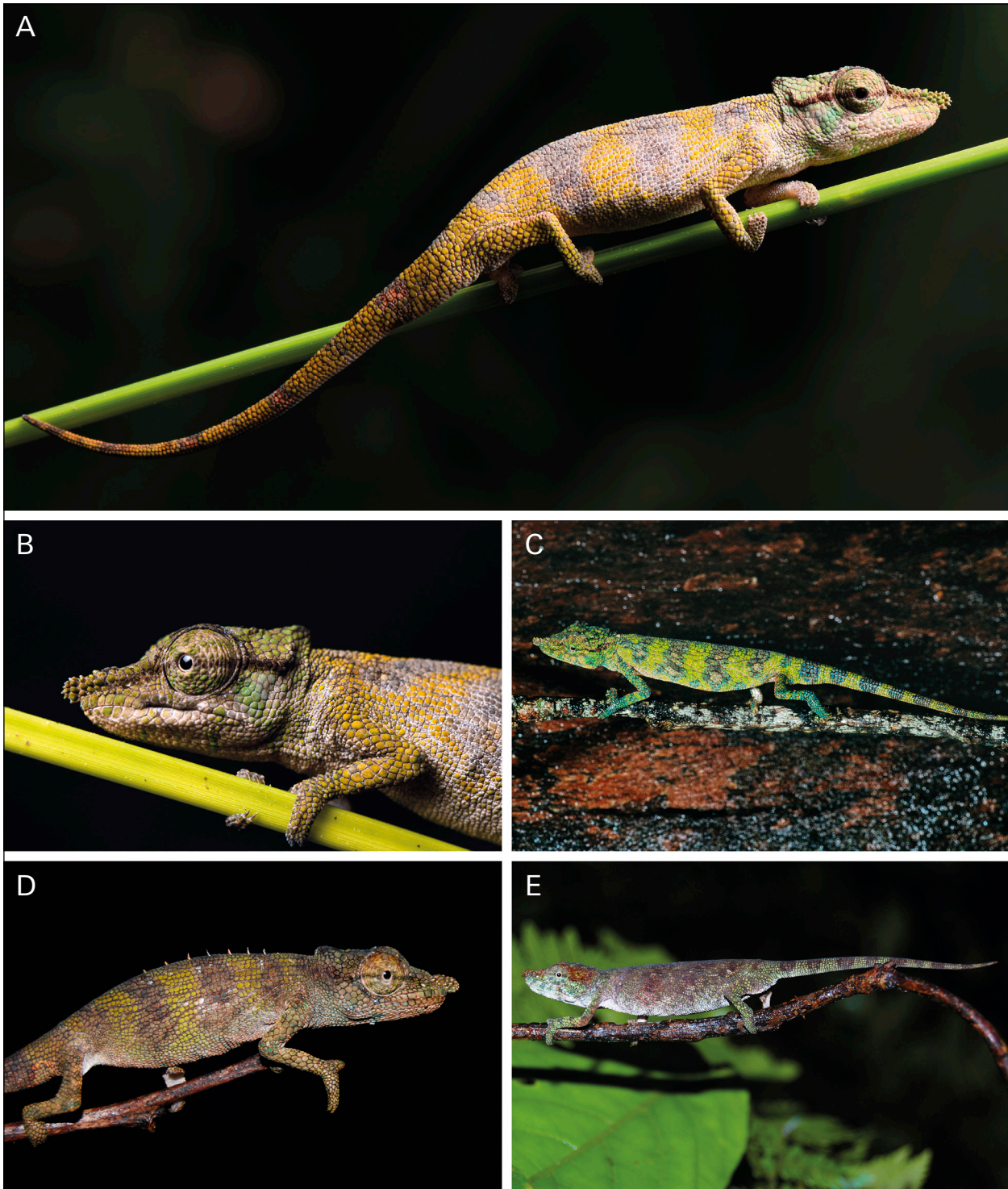


Fig. 13. *Calumma tjiasmantoi* sp. nov. in life. (A, B) adult male (not collected) from Ranomafana NP in relaxed state, photos: M. Knauf; (C) adult male (probably in UADBA) from Andohahela (Camp 2 low elevation) in slightly stressed colouration; (D) adult male and (E) adult female, both from Andreoky, referring to tissue samples PSG_2766, 2768, 2786 in GEHRING *et al.* (2012) in relaxed state, photos: P-S. Gehring.

Distribution (Fig. 9): *Calumma tjiasmantoi* sp. nov. is known from eastern Madagascar from Andohahela in the south to Ranomafana NP about 400 km further north (for coordinates, see above), from an elevation of 267 to 983 m a.s.l. (see Fig. 9).

Identity and re-description of *Calumma fallax* (Mocquard, 1900)

Syntypes: MOCQUARD (1900a, 1900b) did not specify the specimen numbers of the types, but stated that they were one male and one female, collected in Forêt d'Ikongo by Grandidier (MOCQUARD, 1900a). By inference from col-

lection data, we follow BRYGOO (1971), GEHRING *et al.* (2011) and KLAVER (2019) in accepting only two of potentially six specimens as syntypes, MNHN 1899.317, an adult male, and MNHN 1899.318, an adult female, from the locality Forêt d'Ikongo, collected in 1898–1899 by Guillaume Grandidier.

Lectotype designation: We designate MNHN 1899.317, the adult male syntype, as the lectotype of the species, the remaining syntype, MNHN 1899.318, becoming the paralectotype.

Assignment to genetic clade (based on a comparison of the lectotype with the male specimens assigned to clade H, ZSM 693/2003, ZSM 286/2010, ZSM 685/2003, and ZSM 694/2003): *Calumma fallax* belongs to clade H, according to the high casque (2.1 mm in the lectotype vs 1.3–2.5 mm), rounded, oval rostral appendage with a length of (2.7 mm vs 1.8–4.3 mm), heterogeneous scalation in head region with diameter of largest scale in temporal region of 1.6 mm vs 0.8–1.5 mm, distinct parietal crest ending in the casque, temporal crest present consisting of 1 or 2 tubercles (2 vs 1–2); osteology of the skull is almost identical, e.g. width of the frontoparietal fenestra with 16.4% of skull length vs 13.9–15.4%.

Referred material: The specimens MNHN 1890.430, MNHN 1890.431, MNHN 1890.432, all three adult males, and MNHN 1888.24, adult female, are non-type specimens. In addition, in anticipation of our conclusions on the taxonomic identity of the species, we here refer the following specimens to *C. fallax* as it is here re-defined: ZSM 685/2003 (FG/MV 2002-0291), ZSM 693/2003 (FG/MV 2002-0317) and ZSM 694/2003 (FG/MV 2002-0318), all three adult males, collected in Ranomafana NP, Vohiparara, near Kidonavo bridge (about 21.22°S, 47.37°E, about 1000 m a.s.l.), Vavovavy-Fitovinany Region, eastern Madagascar, on 16–20 January 2003 by F. Glaw, M. Puente, L. Raharivololoniaina, M. Thomas, D.R. Vieites; ZSM 134/2005 (FGZC 2508), female, collected in Andohahela NP (24.5440°S, 46.7141°E, 1548 m a.s.l.), Anosy Region, southeastern Madagascar, on 27 January 2005 by F. Glaw, M. Vences, P. Bora; ZSM 286/2010 (FGZC 4588), adult male, collected east of Tsinjoarivo, between camps 2 and 1 (19.7103°S, 47.8182°E, 1465 m a.s.l.) on 23 April 2010 by F. Glaw, J. Köhler, P.-S. Gehring, J.L. Brown, E. Rajeriarison; ZSM 313/2006 (ZCMV 2930), adult female, collected in Ranomafana NP, Vohiparara river and stream/swamp (about 21.25°S, 47.40°E, about 1100 m a.s.l.) on 20 February 2006 by M. Vences, E. Rajeriarison, Y. Chiari, E. Balian; ZSM 476/2010 (FGZC 4352), adult female, collected in Anjozorobe region, Mananara Lodge (18.4629°S, 47.9381°E, 1298 m a.s.l.), Analamanga Region, eastern Madagascar, on 6 April 2010, ZSM 479/2010 (FGZC 4575), adult female, collected east of Tsinjoarivo, camp 1 (19.6800°S, 47.7706°E, 1607 m a.s.l.) on 19 April 2010, both by F. Glaw, J. Köhler, P.-S. Gehring, M. Pabijan, K. Mebert, E. Rajeriarison, F. Randrianasolo, S. Rasamison; ZSM 149/2016 (FGZC 5226) and ZSM 150/2016 (FGZC 5225), both adult females, collected in Mandraka (18.9122°S, 47.9144°E, 1235 m a.s.l.), Analamanga Region, eastern Madagascar, on 5 January 2016 by F. Glaw, D. Prötzel, L. Randriamanana; ZSM 258/2016 (FGZC 5291), adult female, collected in Mandraka (18.9133°S, 47.9145°E, 1260 m a.s.l.) on 3 August 2016 by F. Glaw, D. Prötzel, J. Forster, N. Raharinoro.

Diagnosis (based on the type series and the referred material, see above; osteology based on micro-CT scans of MNHN 1899.317, MNHN 1890.430, ZSM 693/2003, and

ZSM 286/2010, all four males): *Calumma fallax* is characterised by (1) a medium size (male SVL 42.9–50.6 mm, female SVL 40.8–50.7 mm; male TL 90.9–107.3 mm, female TL 77.3–99.8 mm), (2) a long (1.8–4.3 mm in males, 1.7–3.2 mm in females) and distally rounded rostral appendage, (3) rostral scale not integrated into the rostral appendage, (4) prominent rostral crest forming a concave cup on the snout, (5) lateral crests present, (6) temporal crest generally present, (7) cranial crest generally absent, (8) parietal crest generally present but short, (9) a distinctly raised casque in males with a height of 1.3–2.5 mm, (10) a dorsal crest of 6–11 cones in males, generally absent in females (one specimen with five cones), (11) 10–16 supralabial scales with a straight upper margin, (12) absence of axillary pits, (13) diameter of the largest scale in the temporal region of the head 0.8–1.8 mm, (14) a frontoparietal fenestra in the skull, (15) parietal and squamosal generally in contact, (16) parietal bone width at midpoint 6.7–15.7% of skull length, (17) a generally greenish, greyish, or brownish body colouration, (18) a typically blue or grey nose in non-stressed colouration, (19) a green cheek colouration, (20) three blue dorsoventral stripes on the body and a white lateral stripe, and (21) a diffuse brown strip crossing the eye.

C. fallax can be distinguished from all species of the *C. boettgeri* complex (see above) by the absence of occipital lobes; from *C. gallus* by different length, shape and colour of its rostral appendage (see above); from all other species of the *C. nasutum* group without occipital lobes (except for *C. ratnasariae*, see below) by the presence of a frontoparietal fenestra.

In addition, it can be distinguished from *C. vatosoa* by the presence of a rostral appendage (vs absence); from *C. vohibola* by longer rostral appendage (RRS 4.2–8.5% vs 0.2–3.1%), supralabials with a straight upper margin (vs serrated), parietal crest generally present (vs absent); from *C. nasutum* as here redefined by general absence of cranial crest (vs present), a shorter frontal (39.4–50.4% of skull length vs 51.2–82.1%), blue rostral appendage (vs brown), and three blue lateral blotches (vs four brown blotches with light spots); from *C. radamanus* by rostral scale not integrated into the rostral appendage (vs generally integrated), parietal crest generally present (vs absent), supralabials with a straight upper margin (vs serrated), parietal and squamosal in contact or closely approaching (vs widely separated), and width of parietal at midpoint (6.7–15.7% vs 16.1–22.4%); from *C. emelinae* sp. nov. by general presence of parietal crest (vs general absence), higher casque in males (1.3–2.5 mm vs 0.5–1.1 mm), dorsal crest consisting of cones (vs spines) in males, and larger temporal scale in males (0.8–1.6 mm vs 0.7 mm); from *C. tjiasmantoi* sp. nov. by fewer supralabials (10–15 vs 15–17), larger diameter of temporal scale (1.0–1.8 mm vs 0.6–0.8 mm), and slightly narrower postparietal process.

Re-description of the lectotype (Fig. 4E): Adult male, with mouth slightly opened, in good state of preservation, hemipenes not everted. SVL 42.9 mm, tail length

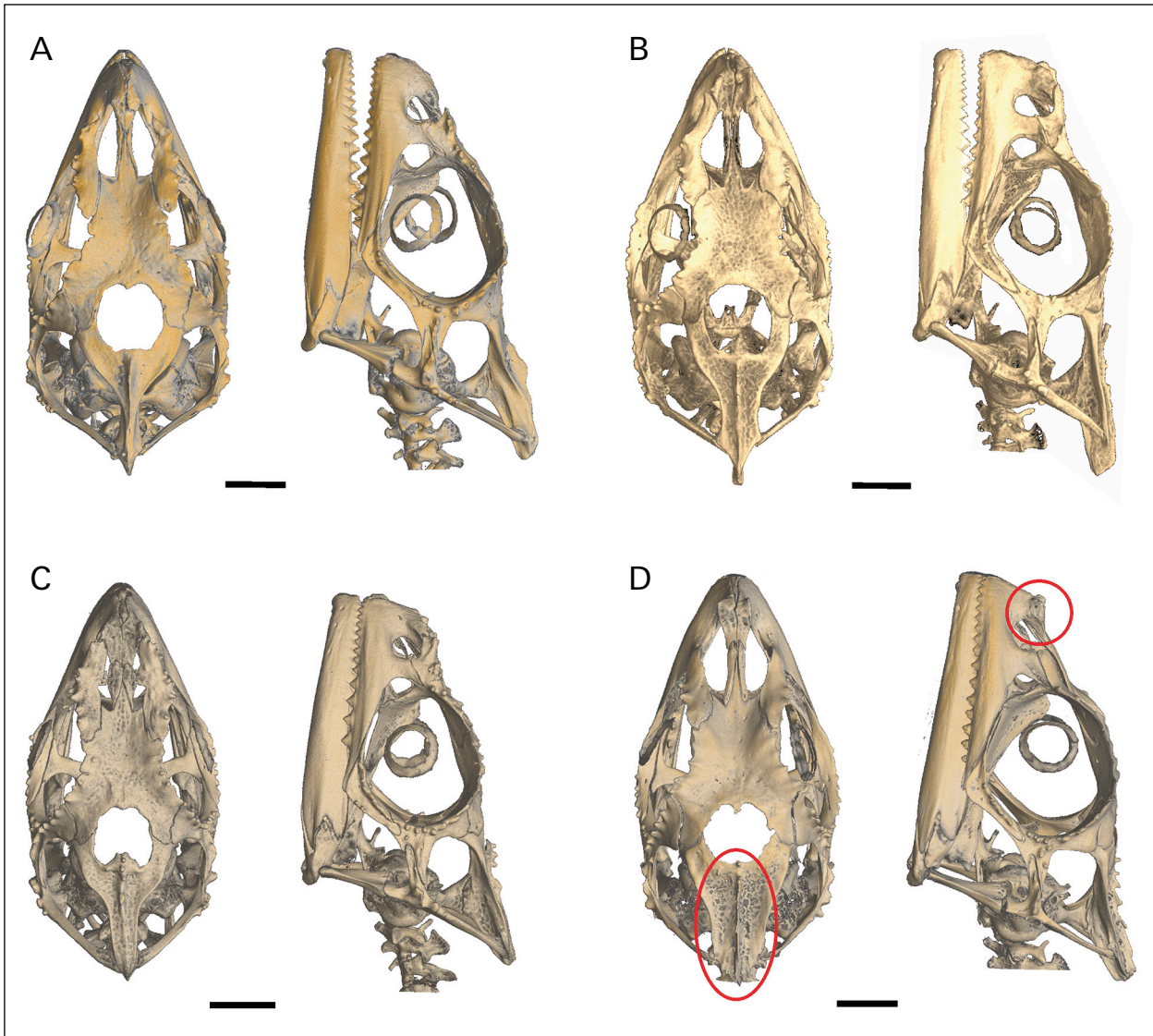


Fig. 14. Micro-computed tomography scans of the skulls of species with a frontoparietal fenestra in dorsal and lateral view. **(A)** *Calumma fallax* (MNHN 1899.317), male lectotype; **(B)** *C. fallax* (MNHN 1840.430), male; **(C)** *C. fallax* (ZSM 286/2016), male of genetic clade H, assigned to *C. fallax*; **(D)** *C. ratnasariae* sp. nov. (ZSM 35/2014), male holotype. Diagnostic characters are encircled in red. Scale bars: 2.0 mm.

53.2 mm, for other measurements, see suppl. Table 1; distinct rostral ridges that render the dorsal surface of the snout a concave cup, laterally compressed dermal rostral appendage of oval tubercle scales that projects straight forward over a length of 2.7 mm with a diameter of 3.4 mm, oblong but taller than wide; 11 infralabial and 11 supralabial scales, all relatively large; supralabials with a smooth dorsal margin; distinct lateral crest running horizontally; distinct temporal crest consisting of two tubercles per side; no cranial crest; distinct parietal crest; no occipital lobes; highly elevated (2.1 mm) and rather acute casque; dorsal crest present, consisting of 11 cones that decrease in height posteriorly; no traces of gular or ventral crest. Body laterally compressed with fine homogeneous scalation and distinctly larger scales on extremities and head region, largest scale in temporal region with diameter of 1.6 mm and in cheek region of 1.4 mm; no axillary or inguinal pits.

Skull osteology of the lectotype (Fig. 14A): Skull length 12.0 mm; snout-casque length 14.6 mm; narrow paired nasals completely separated from each other by the anterior tip of frontal that meets the premaxilla; prefrontal fontanelle and naris fused; prominent prefrontal with laterally raised tubercles exceeding more than the half of the prefrontal fontanelle; frontal and parietal smooth without any tubercles; frontal with a width of 2.7 mm (22.5% of skull length) at border to prefrontal extending to 4.4 mm (36.7%) at border to postorbitofrontal; large frontoparietal fenestra with a width of 2.4 mm (20.0%); curved parietal tapering strongly from a width of 3.9 mm (32.5%) at the border to postorbitofrontal to a width at midpoint of 0.8 mm (6.7%) and broadening slightly posterodorsally, where it is in weak contact with the squamosals; squamosals thin without any tubercles. For further measurements, see Table 2.

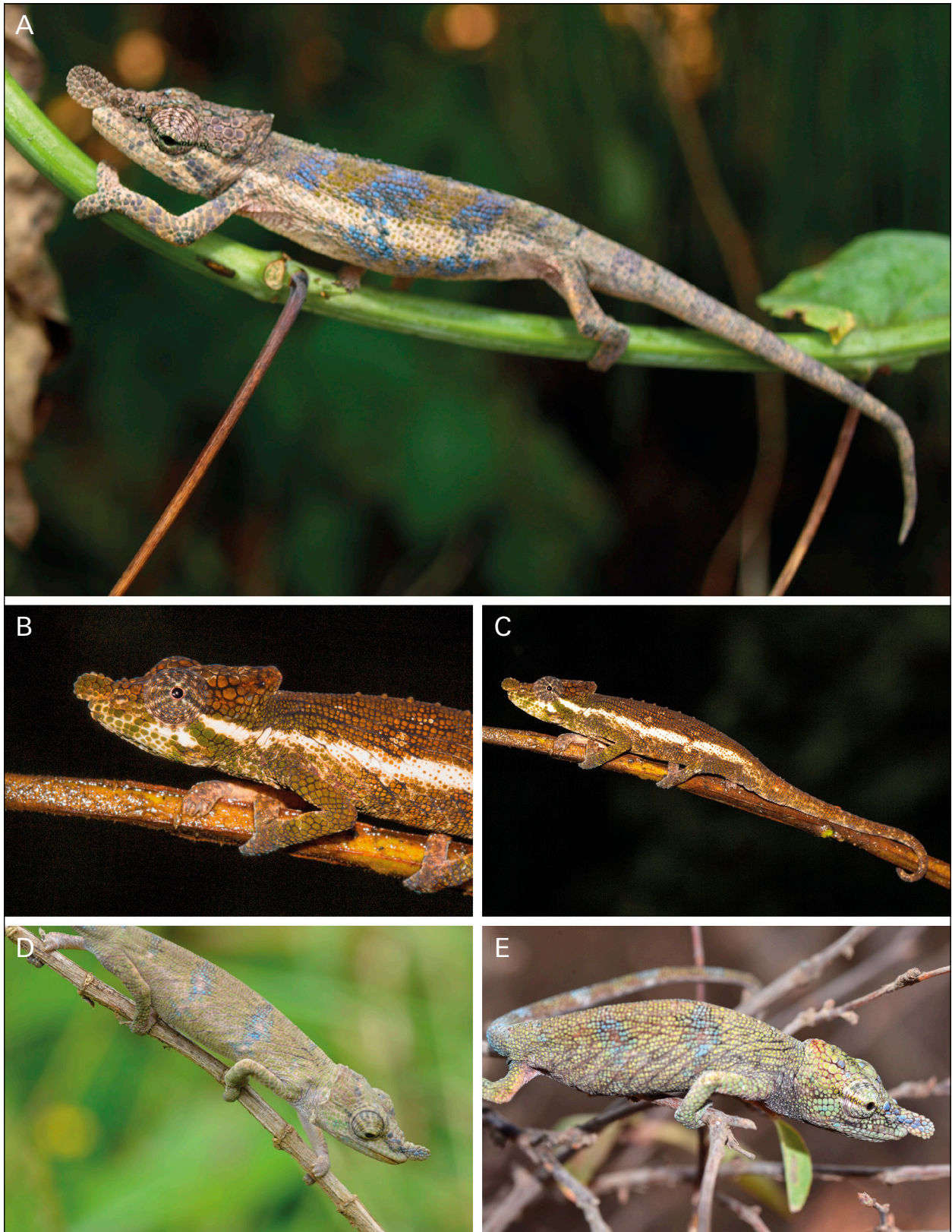


Fig. 15. *Calumma fallax* from different locations. (A) Adult male (not collected) from Tsinjoarivo in relaxed state; (B, C) adult male (not collected) from Ranomafana NP, relaxed, photos: A. Laube/T. Negro; (D, E) both adult females (ZSM 149/2016 and ZSM 258/2016) from Mandraka, relaxed.

Hemipenial morphology, based on the lectotype (no micro-CT scan available): small sized calyces (hemipenial character A); two pairs of finely denticulated rotu-

lae of different size, on sulcal side large with about 16 tips, on asulcal side small with about 8 tips (B); papillary field of few, unpaired papillae (C); pair of medium sized

cornucula gemina (D), only visible when hemipenis fully everted.

Variation: The osteology of the male ZSM 693/2003 differs from the other specimens in having the parietal and squamosal bone not connected; probably this is due to its juvenile state. For variation in measurements, see Table 1. Sexual dimorphism: Body size (SVL and TL) is slightly larger in males than females. Tail length is longer in males than in females (RTaSV 102–124% vs 89–104%). Relative rostral appendage length does not differ. Dorsal crest is more pronounced in males than females.

Colouration in life (Fig. 15): Weak sexual dichromatism, males slightly more colourful. In both sexes grey/beige body colouration with three bright blue dorsoventral stripes on the body that can be crossed by a broad white lateral stripe; extremities and tail of same colour as the body, tail in males can be diffusely annulated; rostral appendage grey or blue; cheek region can be bright green; a diffuse brown stripe may cross the eye.

Etymology: A Latin adjective meaning ‘deceptive’ or ‘fallacious’ in the neutral nominative, with unclear justification.

Distribution (Fig. 9): *Calumma fallax* as redefined here, occurs in eastern Madagascar from Andohahela in the south to Mandraka about 650 km further north (coordinates, see above), from an elevation of 922–1781 m a.s.l.

Description of *Calumma ratnasariae* sp. nov.

ZOOBANK urn:lsid:zoobank.org:act:D822D6EA-7CB8-425B-9AD1-473D1DCFB2C8

Remark: This new species refers to clade I of Fig. 2 and GEHRING *et al.* (2012).

Holotype: ZSM 35/2016 (MSZC 0066), adult male, collected in the Ampotsidy mountains (14.4146°S, 48.7115°E, 1400 m a.s.l.), Sofia Region, northern Madagascar, on 22 December 2015 by M.D. Scherz, J. Borrell, L. Ball, T. Starnes, T.S.E. Razafimandimby, D.H. Nomenjanahary, J. Rabearivony.

Paratypes: ZSM 1724/2010 (ZCMV 12483), adult male and ZSM 2884/2010 (ZCMV 12273), adult female, both collected in Analabe Forest, near Antambato village (Ambodimanga mountain, 14.5048°S, 48.8760°E, 1361 m a.s.l.) on 24 June 2010, ZSM 517/2014 (DRV 6283), adult male collected in Andrevorevo (14.3464°S, 49.1028°E, 1717 m a.s.l.), Sofia Region, northern Madagascar on 21 June 2010, all three by M. Vences, D.R. Vieites, R.D. Randrianiaina, F.M. Ratoavina, S. Rasamison, A. Rakotoarison, E. Rajeriarison, T. Rajoafiarison; ZSM 36/2016 (MSZC 0140), adult female, collected on the Ampotsidy mountains (14.4099°S, 48.7155°E, 1647 m a.s.l.) on 3 January 2016, and ZSM 37/2016 (MSZC 0169), adult female, collected on the Ampotsidy mountains (14.4193°S, 48.7193°E, 1337 m a.s.l.), on 8 January 2016, both by M.D. Scherz, J. Borrell, L. Ball, T.S.E. Razafimandimby, D.H. Nomenjanahary, J. Rabearivony.

Diagnosis (based on the type series; osteology based on micro-CT scans of ZSM 35/2016 and ZSM 517/2014,

both males): *Calumma ratnasariae* sp. nov. is characterised by (1) a large size (male SVL 43.9–52.0 mm, female SVL 48.7–51.5 mm; male TL 97.1–110.7, female TL 95.3–101.0); (2) a short (1.8–2.3 mm in males, 2.1–2.2 mm in females) and distally rounded rostral appendage, (3) rostral scale not integrated into the rostral appendage, (4–7) rostral, lateral, temporal (one tubercle on either side), and cranial crests present, (8) parietal crest distinct and running the length of the parietal bone, (9) a distinctly raised casque in males with a height of 1.3–1.5 mm, (10) a dorsal crest of 7–12 cones in males, generally present in females (6–8 cones), (11) 10–13 supralabial scales with a straight upper margin, (12) absence of axillary pits, (13) diameter of the largest scale in the temporal region of the head 1.2–1.6 mm, (14) a frontoparietal fenestra in the skull, (15) parietal and squamosal in contact (n=2), (16) parietal bone width at midpoint 17.8–18.5% of skull length, (17) a generally yellowish body colouration in males, greyish body colouration in females, (18) rostral appendage not accentuated from the body colouration, (19) a blue and yellow cheek colouration, (20) yellow in males and beige in females, and (21) brown stripe crossing the eye. *Calumma ratnasariae* sp. nov. is unique among the *C. nasutum* complex in having an elevated bony knob on the anterodorsal edge of the maxillary facial process (this character is similar to that seen in *C. uetzi*).

Calumma ratnasariae sp. nov. can be distinguished from all species of the *C. boettgeri* complex (see above) by the absence of occipital lobes; from *C. gallus* by different length, shape and colour of its rostral appendage (see above); from all other species of the *C. nasutum* group without occipital lobes except *C. fallax* by the presence of a frontoparietal fenestra. It is also quite unusual in having an overall yellowish body colouration in males. In addition, it can be distinguished from *C. vatsoa* easily by the presence of a rostral appendage (vs absence); from *C. vohibola* by longer rostral appendage (RRS 3.8–4.8% vs 0.2–3.1%), parietal crest present (vs absent), fewer supralabials (10–13 vs 13–16) with a straight upper margin (vs serrated), larger temporal scale (1.2–1.6 mm vs 1.0 mm), broader parietal bone with a continuous parietal crest (vs smooth parietal); from *C. nasutum* as here redefined by a larger maximum total length in males (110.7 mm vs 89.0–100.8 mm), a distinct parietal crest (vs absent or indistinct), dorsal crest generally present in both sexes (vs generally absent and absent in females); from *C. radamanus* by larger total length (95.3–110.7 mm vs 77.0–93.5 mm), tail length in males longer than SVL (vs shorter), rostral scale not integrated into the rostral appendage (vs generally integrated), parietal crest present (vs absent), supralabials with a straight upper margin (vs serrated), larger temporal scale (1.2–1.6 mm vs 0.6–0.9 mm), and parietal and squamosal in contact (vs widely separated); from *C. emelinae* sp. nov. by parietal crest distinct (vs general absence), higher casque in males (1.3–1.5 mm vs 0.5–1.1 mm), dorsal crest consisting of cones (vs spines) in males; larger temporal scale (1.2–1.6 mm vs 0.6–1.0 mm), and



Fig. 16. *Calumma ratnasariae* sp. nov. from Ampotsidy mountains. (A, B) Adult male holotype (ZSM 35/2016), slightly displaying, and (C) adult female (MSZC 0130, UADBA uncatalogued) in relaxed state.

broad postparietal process (vs strongly tapering); from *C. tjiasmantoi* sp. nov. by larger body length of females (SVL 48.7–51.5 mm vs 43.9–46.1 mm), dorsal crest generally present in females (vs absent), fewer supralabials (11–12 vs 15–17), and larger diameter of temporal scale (1.2–1.6 mm vs 0.6–0.8 mm); and from *C. fallax* by generally shorter relative rostral appendage length in females (RRS 4.1–4.5% vs 4.2–7.6%), cranial crest present (vs generally absent), parietal crest longer and more distinct, dorsal crest generally present in females (vs generally absent), and a wider mid-parietal width (17.8–18.5% of skull length vs 6.7–15.7%).

Description of the holotype (Figs. 4F, 16 A,B): Adult male, with mouth closed, in good state of preservation, with everted hemipenes, one completely (on the left) and one incompletely (on the right); SVL 48.2 mm, tail length 54.2 mm, for other measurements, see suppl. Table 1; distinct rostral ridges that give the snout a right angle; later-

ally compressed dermal rostral appendage of oval tubercle scales that projects slightly downwards over a length of 2.3 mm with a diameter of 1.9 mm; 13 infralabial and 12 supralabial scales, both relatively large; supralabials with a smooth dorsal margin; distinct lateral crest running horizontally; temporal crest consisting of one tubercle per side; short cranial crest; distinct and long parietal crest ending in the tip of the casque with a height of 1.5 mm; no occipital lobes; dorsal crest present, consisting of 7 broad cones; no traces of gular or ventral crest. Body laterally compressed with fine homogeneous scalation and distinctly larger scales on extremities and head region, largest scale in temporal region with diameter of 1.3 mm and in cheek region of 1.1 mm; no axillary or inguinal pits.

Skull osteology of the holotype (Fig. 14D): Skull length 11.9 mm; snout-casque length 14.4 mm; narrow paired nasals anterior slightly connected; anterior tip of frontal exceeding the middle of the prefrontal fontanelle, which

is fused with the naris; prominent and broad prefrontal; frontal and parietal smooth without any tubercles; frontal with a width of 2.6 mm (21.8% of skull length) at border to prefrontal extending to 4.4 mm (37.0%) at border to postorbitofrontal; large frontoparietal fenestra with a width of 2.5 mm (21.0%); broad parietal with distinct parietal crest tapering slightly from a width of 4.0 mm (33.6%) at the border to postorbitofrontal to a width at midpoint of 2.2 mm (18.6%); the posterodorsally broadened end is in weak contact with the squamosals; squamosals thin with a few tubercles. For further measurements, see Table 2.

Hemipenial morphology, based on ZSM 1724/2010 (Fig. 5E), ZSM 517/2014, and ZSM 35/2016: small calyces (hemipenial character A); two pairs of finely denticulated rotulae of different size, on sulcal side large with about 12–15 tips, on asulcal side small with about 5–7 tips (B); papillary field of small, unpaired papillae (C); pair of short cornucula gemina (D), only visible when hemipenis fully everted.

Variation: For variation in measurements, see Table 1. Sexual dimorphism: Males and females do not seem to differ in body size. Tail length is longer in males than in females (RTaSV 112–121% vs 94–98%). Relative rostral appendage length does not differ. Dorsal crest does not differ between males and females.

Colouration in life (Fig. 16): Strong sexual dichromatism with males of yellow body colouration and turquoise stripes and females generally uniformly beige. Males with turquoise annulated tail and extremities and two brown blotches on the body side that is crossed by a diffuse white lateral stripe; no pattern in females; throat and ventral region slightly brighter than the flank; indistinct rostral appendage not accentuated from the body/head, can be spotted with blue or yellow dots; in males cheek region and eyelids with turquoise dots, in females blue dots can occur on rostral ridges and eyelids when stressed; a diffuse brown stripe crosses the eye in both sexes.

Etymology: The specific epithet is named after Yulia Ratnasari, in recognition of her support for taxonomic research and nature conservation projects in Madagascar through the BIOPAT initiative (<http://biopat.de/en/>).

Distribution (Fig. 9): *Calumma ratnasariae* sp. nov. is only known from the Bealanana District of northern Madagascar. It is distributed from Analabe Forest in the south to Andrevorevo, about 20 km further north (for coordinates, see above), from an elevation of 1337–1717 m a.s.l.

Key for male specimens of the *Calumma nasutum* group

The following key is based on external morphology only and some characters of species lacking occipital

lobes (highlighted by underlined numbers, except for *Calumma roaloko*) are illustrated in Fig. 17 with numbers referring to the sections of the key. For diagnostic characters of colouration, see Table 4, and for further morphological characters, see Table 1. Females of this complex are more homogeneous in morphology and thus generally show fewer diagnostic characters (e.g. shorter and indistinct rostral appendages, usually lacking a dorsal crest) and were not considered in the identification key, except for the identification of *C. juliae* where only females are known so far. The key for the *Calumma boettgeri* complex of PRÖTZEL *et al.* (2018b) was modified and supplemented with *C. roaloko*. Illustrations of characters for underlined numbers in the key are given in Fig. 17.

- 1a** Occipital lobes absent (*Calumma nasutum* complex) **2**
- 1b** Occipital lobes present (*Calumma boettgeri* complex) **9**
- 2a** Rostral appendage long (5.0–11.0 mm) and spear-like, dorsal crest absent, homogeneous scalation on body and head **Calumma gallus complex**
- 2b** Rostral appendage shorter and rounded, dorsal crest can be present or absent, more or less heterogeneous scalation on body and head **3**
- 3a** Rostral scale integrated in rostral appendage, rostral appendage oriented downwards, parietal crest absent, absence of cornucula gemina on hemipenis
..... **Calumma radamanus complex**
- 3b** Rostral scale not integrated in rostral appendage, rostral appendage straight or oriented upwards, parietal crest present (can be absent in *C. nasutum* and *C. vohibola*), cornucula gemina present **4**
- 4a** Rostral appendage short (≤ 1.4 mm), small total length (≤ 89.0 mm), dorsal crest present and consisting of spines **Calumma vohibola**
- 4b** Rostral appendage completely lacking, large total length (> 120.0 mm), dorsal crest absent.....
..... **Calumma vatosa**
- 4c** Rostral appendage longer (> 1.4 mm), total length medium sized (89.0–110.0 mm), dorsal crest present or absent..... **5**
- 5a** Low casque (≤ 0.6 mm) and dorsal crest consisting of spines **Calumma emelinae sp. nov.**
- 5b** Casque higher (> 0.6 mm) and dorsal crest consisting of small cones, if present (spines can also occur in *C. radamanus* and *C. vohibola*) **6**
- 6a** Casque height < 1.5 mm **7**
- 6b** Casque height > 1.5 mm **8**
- 7a** Relatively homogeneous scalation on the head with diameter of largest temporal scale ≤ 0.8 mm, high number of supra- and infralabial scales ($n \geq 15$), frontoparietal fenestra absent (you can feel the closed skull roof by gently pushing the top of the head of a preserved specimen)
..... **Calumma tjiasmantoi sp. nov.**
- 7b** Heterogeneous scalation on the head with diameter of largest temporal scale ≥ 1.3 mm, lower number of

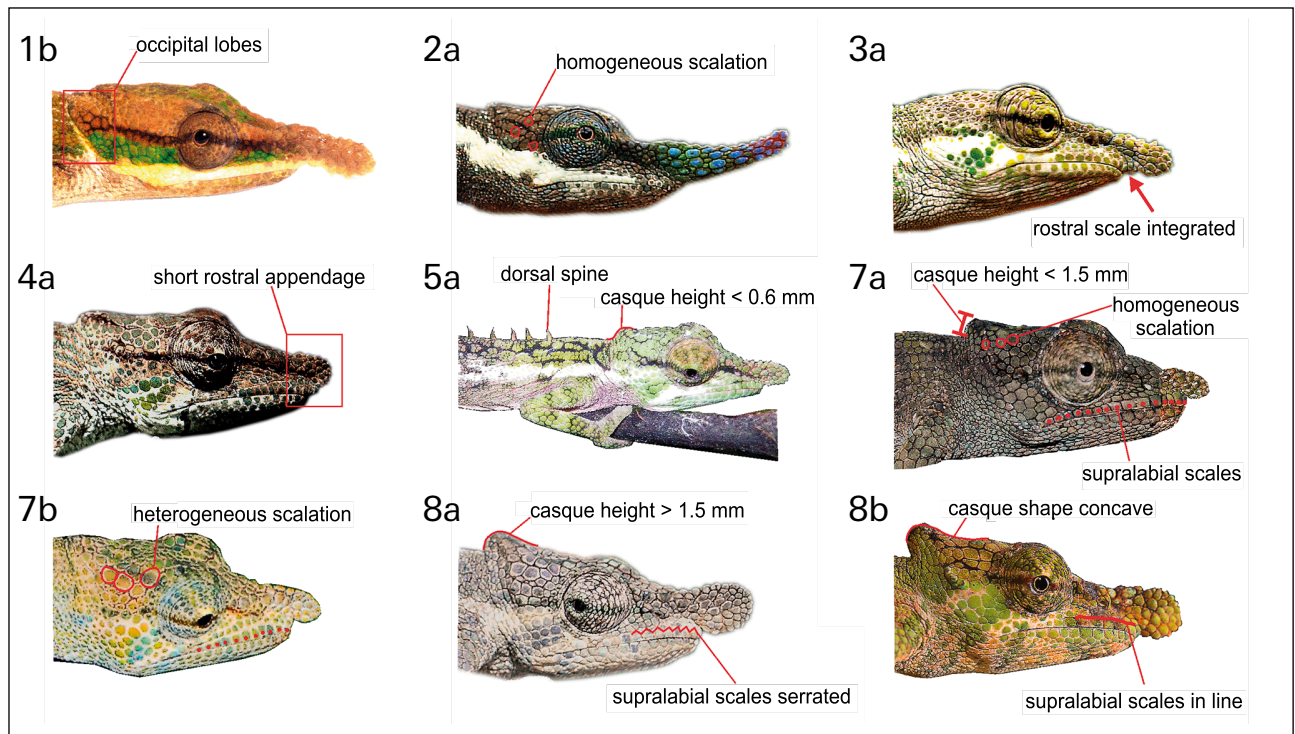


Fig. 17. Illustrations of important characters of the identification key to the species of the *Calumma nasutum* complex lacking occipital lobes (except for *C. roaloko*, illustrated in 1b). The numbers in the upper left refer to the respective sections of the identification key. Diagnostic characters are marked in red. For further diagnostic characters, see also Table 1.

- supra- and infralabial scales (10–14), frontoparietal fenestra present (the top of the head of a preserved specimen feels soft) ... *Calumma ratnasariae* sp. nov.
- 8a** Parietal crest present, frontoparietal fenestra present, casque rather rounded (convex), axillary pits absent, upper margin of supralabial scales usually serrated *Calumma fallax*
- 8b** Parietal crest usually absent, frontoparietal fenestra absent, casque rather pointed (concave), axillary pits can occur, upper margin of supralabial scales usually in line *Calumma nasutum*
- 9a** Small tubercle scales (diameter ≤ 0.5 mm) on extremities, small body size (< 110 mm total length, ≤ 45 mm SVL) **10**
- 9b** Large tubercle scales (diameter 0.5–0.9 mm) on extremities, large body size (generally > 110 mm total length, > 45 mm SVL) **12**
- 10a** Tubercle scales on extremities isolated from each other, upper margin of supralabial scales serrated... *Calumma boettgeri*
- 10b** Tubercle scales on extremities bordering each other, upper margin of supralabial scales in line **11**
- 11a** Temporal crest present, dorsal crest consisting of 13–14 cones or spines, medium sized rostral appendage (≤ 3.9 mm) *Calumma uetzi*
- 11b** Temporal crest absent, dorsal crest consisting of 1–2 cones, longer rostral appendage (≥ 3.9 mm).... *Calumma roaloko*
- 12a** Occipital lobes not or only slightly separated (notch 0–0.8 mm), no frontoparietal fenestra (closed skull roof) **13**
- 12b** Occipital lobes clearly separated (notch > 0.5 mm), frontoparietal fenestra present (can be felt through the skin in alcohol-preserved specimens) **14**
- 13a** Temporal crest of one or two tubercles present, parietal crest present, dorsal crest in females absent or consisting of up to 6 dorsal cones *Calumma linotum*
- 13b** Temporal crest absent, parietal crest absent, dorsal crest present in females and consisting of 9–14 cones *Calumma juliae*
- 14a** Large frontoparietal fenestra, occipital lobes widely separated, dorsal and caudal crest absent, rostral appendage rounded *Calumma guibei*
- 14b** Small frontoparietal fenestra, occipital lobes slightly connected, dorsal crest of 7–15 distinct cones, no caudal crest, rostral appendage rounded *Calumma gehringi*
- 14c** Medium-sized frontoparietal fenestra, occipital lobes completely separated, dorsal crest of > 20 small conical scales, caudal crest present, rostral appendage pointed > 5.5 mm *Calumma lefona*

Discussion

As already suggested by GEHRING *et al.* (2012), *Calumma nasutum* has turned out to be a complex of several species. Excluding the OTUs assigned to the *C. boettgeri* complex and *C. gallus* complex, GEHRING *et al.* (2012) calculated six OTUs within *C. fallax* (OTUs 17–21, plus

Table 4. Diagnostic characters of the *Calumma nasutum* group based on colouration. f, female; m, male; further abbreviations see Material and Methods.

species	sex	colouration of body	colouration of rostral appendage	colouration of the cheek	body patterning	stripe crossing the eyes
		17	18	19	20	21
<i>C. nasutum</i>	m	brown, green, yellowish	= body colouration	= body colouration	three to four diffuse brown dorsoventral blotches of variable colour and a light lateral stripe	indistinct brown stripe
<i>C. nasutum</i>	f	green to beige	= body colouration	= body colouration	four diffuse brown dorsoventral blotches with light spots on the body and a light lateral stripe	indistinct brown stripe
<i>C. radamanus</i>	m	green to beige	turquoise or blue	turquoise or bright green	three blue or violet lateral blotches, crossed by a beige-white stripe	brown stripe
<i>C. radamanus</i>	f	green to beige	turquoise or blue	turquoise or bright green	three blue or violet lateral blotches, crossed by a beige-white stripe	brown stripe
<i>C. emelinae</i> sp. nov.	m	green to beige	= body colouration	bright green	three scattered black blotches and white lateral stripe	black stripe
<i>C. emelinae</i> sp. nov.	f	brown to beige	indistinct green or blue	bright green	no pattern	indistinct black stripe
<i>C. ifiasmantoi</i> sp. nov.	m	bright green, yellowish	= body colouration	turquoise	five diffuse blotches	indistinct brown stripe
<i>C. ifiasmantoi</i> sp. nov.	f	brown	= body colouration	= body colouration	five diffuse blotches	indistinct brown stripe
<i>C. fallax</i>	m	grey/beige	grey or blue	grey or bright green	three bright blue stripes	indistinct grey stripe
<i>C. fallax</i>	f	grey/beige	grey or blue	grey or bright green	three bright blue stripes	indistinct grey stripe
<i>C. ratnasariae</i> sp. nov.	m	yellow	= body colouration or blue	turquoise	two brown blotches and lateral stripe	brown stripe
<i>C. ratnasariae</i> sp. nov.	f	beige	= body colouration or blue	= body colouration	none	brown stripe

‘*C. fallax*’) and even twelve OTUs (6, 7, 13–16, 22–26, plus ‘*C. nasutum*’) that formerly were all treated as the single species *C. nasutum*. The OTUs in that study were calculated using three different approaches (net p-distances, SpeciesIdentifier and GMYC model) all based on divergences of a ND2 gene fragment. Using integrative taxonomy we here consider most of the 18 OTUs ‘within’ the two described species as intraspecific diversity. However, the classification into different clades based on ND2 divergences of > 8.2% proved to be a helpful orientation to evaluate taxonomic units. Following our integrative revision, the clades B, G, H, I, J, and K have resulted in one species each. The 18 OTUs from GEHRING *et al.* (2012) constitute six species, three of which we have described herein, and one of which we have resurrected. For the whole *C. nasutum* group (including the *C. boettgeri* complex but excluding the *C. gallus* complex) GEHRING *et al.* (2012) calculated a total of 27 OTUs that have resulted in 12 described species to date, not considering the recently discovered species *C. juliae*, *C. uetzi*, and *C. roaloko* (PRÖTZEL *et al.*, 2018a), which were not yet studied by GEHRING *et al.* (2012). This fits the general pattern of overestimation of species numbers based on species delimitation algorithms (LEACHÉ *et al.*, 2019).

In some known lizard cases, mitochondrial divergence (COI, cytochrome *b* and ND2) can exceed 10% between apparently conspecific populations of anole lizard species (JACKMAN *et al.*, 2002; THORPE *et al.*, 2005). The comparison of different groups of chameleons confirms also the phenomenon that morphological and mitochondrial variation or differentiation are not necessarily correlated, as shown e.g. in *Anolis roquet* on Martinique (THORPE *et al.*, 2008; LOSOS, 2009). The deep mitochondrial lineages within the *C. nasutum* group, which is morphologically rather conserved, contrasts for example with species within the genus *Bradypodion* where some morphologically distinct species differ genetically by just 5% or less in the ND2 gene (BRANCH *et al.*, 2006; TILBURY & TOLLEY, 2009).

We reiterate the importance of an integrative approach in taxonomy, making use of as many methods as possible. MIRALLES *et al.* (2011) and VASCONCELOS *et al.* (2012) for example used three lines of evidence (mtDNA, nDNA, and morphology) and described a species if at least two lines showed clear differences. In the present work we took advantage of emerging methods in taxonomy, and additionally used micro-CT scans for skull morphology and diceCT scans (GIGNAC *et al.*, 2016) for detailed hemipenial morphology. Most of the chameleon species described here differ in four (mtDNA, nDNA, external morphology, and skull osteology) of five lines of evidence; of these, only the morphology of the hemipenis shows a limited amount of variation in the *C. nasutum* group. Yet, in *C. radamanus*, the hemipenes have larger calyces and are lacking the cornucula gemina (PRÖTZEL *et al.*, 2017), which makes the species unique in all five lines of evidence. Other characters show a great variability, such as the dorsal crest, which can be present or absent in males of *C. linotum* (PRÖTZEL *et al.*, 2015), *C. nasutum*, *C. radamanus*, or *C. vohibola* (GEHRING *et al.*, 2011). More constant is the shape of the dorsal crest, consisting either of spines, e.g. in *C. radamanus*, or cones, e.g. in *C. fallax*, and *C. ratnasariae* sp. nov. Another character that is usually diagnostic is the presence or absence of axillary pits (ANDREONE *et al.*, 2001), which are also present in the type se-

ries of *C. nasutum* and were also mentioned by GEHRING *et al.* (2011). Axillary pits are lacking in the specimens of clade K, which *C. nasutum* was assigned to, following GEHRING *et al.* (2012). So far, we cannot tell whether the presence of axillary pits also varies, perhaps depending on the presence or number of mites in the habitat, or if the structure of the skin might have changed during the long period of storage and the axillary pits are artefacts. As mentioned above, the assignment of *C. nasutum* to clade K was partly done owing to the lack of better alternatives and to avoid over-splitting of species. An attempt to isolate DNA from the lectotype using a target enrichment approach in development by STRAUBE *et al.* (unpubl. data) failed, but might be repeated once this promising method is better established. The assignment of *C. fallax* to clade H, again following GEHRING *et al.* (2012), is strongly supported by morphological and osteological characters, e.g. presence of a FF, and also by the knowledge of the type locality, which is in south-eastern Madagascar within the distribution of clade H specimens.

In this work six species of *Calumma* were either re-described, revalidated or newly described and their protection status needs to be updated. The IUCN distribution map of *Calumma nasutum*, for example, shows this species occurring all along the east coast and in northern Madagascar and it is listed as ‘Least Concern’ (JENKINS *et al.*, 2011). Such assessments based on species complexes are a common problem, as they fail to capture the taxonomic uncertainty, and should more reasonably be considered ‘Data Deficient’ until their taxonomy is resolved; see the recent discussion of this topic by SCHERZ *et al.* (2019b). Now that we have resolved this complex, re-assessments are possible. Due to the alignment of the species to clade K, *C. nasutum* now has a disjunct distribution of small parts in eastern and northern Madagascar (see Fig. 9) and following the IUCN criteria B1ab(iii), we suggest to classify it as ‘Vulnerable’ (its extent of occurrence is < 20,000 km²). For *C. ratnasariae* we estimate an extent of occurrence of 2500 km², and following the criteria B1ab(iii) again, we suggest that it be given the IUCN status ‘Endangered’. The other four species we would classify as ‘Least Concern’ due to their large ranges, but note that, although they do generally frequent disturbed and open areas within forests, their natural habitat is nevertheless decreasing, and their populations trends are likely to be declining.

With 17 described species to date the *C. nasutum* group is surprisingly diverse compared to other groups within the genus. The species of the *C. furcifer* group for example are of similar body size (PRÖTZEL *et al.*, 2016) and their genetic clades radiated at about the same time (TOLLEY *et al.*, 2013) but the group contains only eight described species to date (GLAW, 2015). Most species of the *C. furcifer* group are morphologically similar to each other, and all are more or less uniformly green in colour and lacking any conspicuous colour signals (except *C. tarzan*, which has remarkable stress colouration; GEHRING *et al.*, 2010). Signalling structures may promote speciation by enhancing sexual selection or species recognition, and in some

lizards it has been hypothesised that signalling structures, e.g. dewlaps in Dactyloidae (anoles), have contributed to increased speciation and diversification rates (LOSOS, 2009; INGRAM *et al.*, 2016). The rostral appendage of the *C. nasutum* group is known to serve a role in intraspecific communication (PARCHER, 1974) and might accelerate the rate of speciation as well. Within the group the prominence of the rostral appendage is highly variable. It ranges from very large in *C. gallus*, *C. gehringi*, and *C. lefona* to almost completely absent in *C. vohibola* or completely absent in *C. vatosoa*. Colour variation of the rostral appendage is also strong, with the appendage being green or blue in *C. gehringi*, violet or green in *C. radamanus*, red or multi-coloured in *C. gallus*, blue in *C. fallax* and *C. linotum*, and yellowish in *C. tjiasmantoi*. In contrast to anoles there are no studies about the signalling function of colour variation of the rostral appendages in chameleons. It would be interesting to figure out whether there is a correlation of the prominence of the rostral appendage with the presence of syntopic species of the group. There is certainly a great deal of potential for future studies on this fascinating group of lizards.

Acknowledgements

We thank N. Straube (ZSM, München) for his efforts to obtain DNA from the *C. nasutum* lectotype, M. Franzen (ZSM, München) for support in the collection and checking specimen numbers, I. Neich (Museum National d’Histoire Naturelle; MNHN, Paris), G. Köhler and L. Acker (Senckenberg Museum, Frankfurt/Main; SMF), W. Böhme and M. Flecks (Zoologisches Forschungsmuseum Alexander Koenig; ZFMK, Bonn), and F. Andreone (Museo Regionale di Scienze Naturali; MRSN, Torino) for the loan of specimens. Further, we are grateful to P.-S. Gehring, M. Knauf, A. Laube and T. Negro for providing photographs and to W. Prötzel and M. Spies for discussion of Latin grammar and nomenclatural issues of *Calumma radamanus*, respectively. We also want to thank everyone who helped collecting in the field, especially the collectors of type specimens (G. Aprea, E. Balian, L. Ball, P. Bora, J. Borrell, J.L. Brown, Y. Chiari, R. Dolch, J. Forster, P.-S. Gehring, K. Glaw, T. Glaw, O. Hawlitschek, J. Köhler, K. Mebert, D.H. Nomenjanahary, M. Pabijan, J. Patton, M. Puente, J. Rabearivony, N. Raharinoro, L. Raharivoloniaina, E. Rajeriarison, T. Rajoafiarison, A. Rakotoarison, J.W. Ranaivosolo, R.D. Randrianiaina, L. Randriamanana, S. Rasamison, T.S.E. Razafimandimby, T. Starnes, M. Thomas, D.R. Vieites). We furthermore thank two anonymous reviewers for their helpful comments on the manuscript. Finally, we thank the Malagasy authorities, in particular the Ministère de l’Environnement et des Forêts for issuing research and export permits, and the German authorities for the import permits.

References

- ANDREONE, F., MATTIOLI, F., JESU, R. & RANDRIANIRINA, J. E. (2001). Two new chameleons of the genus *Calumma* from north-east Madagascar, with observations on hemipenal morphology in the *Calumma furcifer* group (Reptilia, Squamata, Chamaeleonidae). *Journal of Herpetology*, **11**, 53–68.
- ANGEL, F. (1942). Les lézards de Madagascar. *Mémoires de l’Académie Malgache*, **36**, 1–193.

- BICKFORD, D., LOHMAN, D. J., SODHI, N. S., NG, P. K., MEIER, R., WINKER, K., INGRAM, K. K. & DAS, I. (2006). Cryptic species as a window on diversity and conservation. *Trends in Ecology & Evolution*, **22**, 148–155.
- BRANCH, W., TOLLEY, K. A. & TILBURY, C. R. (2006). A new Dwarf Chameleon (Sauria: *Bradypodion* Fitzinger, 1843) from the Cape Fold Mountains, South Africa. *African Journal of Herpetology*, **55**, 123–141.
- BRUFORD, M., HANOTTE, O., BROOKFIELD, J. & BURKE, T. (1992). Single-locus and multilocus DNA fingerprint. In: A. HOELZEL (Ed), *Molecular genetic analysis of populations: a practical approach*. Oxford University Press, Oxford, pp. 225–270.
- BRYGOO, E. R. (1971). Reptiles Sauriens Chamaeleonidae. Genre *Chamaeleo*. *Faune de Madagascar*, **33**, 1–318.
- DORR, L. J. (1997). *Plant collectors in Madagascar and the Comoro Islands*. Kew, Royal Botanic Gardens.
- DUMÉRIL, A. & BIBRON, G. (1836). *Erpétologie Générale ou Histoire Naturelle Complète des Reptiles* (Vol. III). Paris, Librairie encyclopédique de Roret.
- DUMÉRIL, A., BIBRON, G. & DUMÉRIL, A. (1854). *Erpétologie Générale ou Histoire Naturelle Complète des Reptiles. Tome Septième, Deuxième Partie* (Vol. XII). Paris, Librairie Encyclopédique de Roret.
- ECKHARDT, F. S., GEHRING, P.-S., BARTEL, L., BELLMANN, J., BEUKER, J., HAHNE, D., KORTE, J., KNITTEL, V., MENSCH, M., NAGEL, D., POHL, M., ROSTOSKY, C., VIERATH, V., WILMS, V., ZENK, J. & VENCES, M. (2012). Assessing sexual dimorphism in a species of Malagasy chameleon (*Calumma boettgeri*) with a newly defined set of morphometric and meristic measurements. *Herpetology Notes*, **5**, 335–344.
- GEHRING, P.-S., PABIAN, M., RATSOAVINA, F. M., KÖHLER, J., VENCES, M. & GLAW, F. (2010). A Tarzan yell for conservation: a new chameleon, *Calumma tarzan* sp. n., proposed as a flagship species for the creation of new nature reserves in Madagascar. *Salamandra*, **46**, 167–179.
- GEHRING, P.-S., RATSOAVINA, F. M., VENCES, M. & GLAW, F. (2011). *Calumma vohibola*, a new chameleon species (Squamata: Chamaeleonidae) from the littoral forests of eastern Madagascar. *African Journal of Herpetology*, **60**, 130–154.
- GEHRING, P.-S., TOLLEY, K. A., ECKHARDT, F. S., TOWNSEND, T. M., ZIEGLER, T., RATSOAVINA, F., GLAW, F. & VENCES, M. (2012). Hiding deep in the trees: Discovery of divergent mitochondrial lineages in Malagasy chameleons of the *Calumma nasutum* group. *Ecology and Evolution*, **2**, 1468–1479.
- GIGNAC, P. M., KLEY, N. J., CLARKE, J. A., COLBERT, M. W., MORHARDT, A. C., CERIO, D., COST, I. N., COX, P. G., DAZA, J. D. & EARLY, C. M. (2016). Diffusible iodine-based contrast-enhanced computed tomography (diceCT): An emerging tool for rapid, high-resolution, 3-D imaging of metazoan soft tissues. *Journal of Anatomy*, **228**, 889–909.
- GLAW, F. (2015). Taxonomic checklist of chameleons (Squamata: Chamaeleonidae). *Vertebrate Zoology*, **65**, 167–246.
- GLAW, F. & VENCES, M. (1994). *A fieldguide to the amphibians and reptiles of Madagascar* (2nd ed.). Cologne, Vences & Glaw Verlag.
- GLAW, F. & VENCES, M. (2007). *A field guide to the amphibians and reptiles of Madagascar* (3rd ed.). Cologne, Vences & Glaw Verlag.
- HAN, D., ZHOU, K. & BAUER, A. M. (2004). Phylogenetic relationships among gekkotan lizards inferred from C-mos nuclear DNA sequences and a new classification of the Gekkota. *Biological Journal of the Linnean Society*, **83**, 353–368.
- HARPER, G. J., STEININGER, M. K., TUCKER, C. J., JUHN, D. & HAWKINS, F. (2007). Fifty years of deforestation and forest fragmentation in Madagascar. *Environmental Conservation*, **34**, 325–333.
- INGRAM, T., HARRISON, A., MAHLER, D. L., DEL ROSARIO CASTAÑEDA, M., GLOR, R. E., HERREL, A., STUART, Y. E. & LOSOS, J. B. (2016). Comparative tests of the role of dewlap size in *Anolis* lizard speciation. *Proceedings of the Royal Society of London B: Biological Sciences*, **283**, 1–9.
- INTERNATIONAL COMMISSION ON ZOOLOGICAL NOMENCLATURE (1999). *International code of zoological nomenclature*, International Trust for Zoological Nomenclature.
- JACKMAN, T. R., IRSCHICK, D. J., DE QUEIROZ, K., LOSOS, J. B. & LARSON, A. (2002). Molecular phylogenetic perspective on evolution of lizards of the *Anolis grahami* series. *Journal of Experimental Zoology Part A: Ecological Genetics and Physiology*, **294**, 1–16.
- JENKINS, R. K. B., ANDREONE, F., ANDRIAMAZAVA, A., ANJERINIAINA, M., BRADY, L., GLAW, F., GRIFFITHS, R. A., RABIBISOA, N., RAKOTOMALALA, D., RANDRIANANTOANDRO, J. C., RANDRIANIRIANA, J., RANDRIANIZAHANA, H., RATSOAVINA, F. & ROBSOMANITRANDRASANA, E. (2011). *Calumma nasutum*. The IUCN Red List of Threatened Species, e.T172861A6931331.
- KLAVER, C. (2019). Notes on the typification of several chameleon taxa (Sauria: Chamaeleonidae). *Amphibia-Reptilia*, DOI: 10.1163/15685381-20191230.
- KLAVER, C. & BÖHME, W. (1986). Phylogeny and classification of the Chamaeleonidae (Sauria) with special reference to hemipenis morphology. *Bonner Zoologische Monographien*, **22**, 1–64.
- KLAVER, C. & BÖHME, W. (1997). *Chamaeleonidae. Das Tierreich. Part 112*. Berlin and New York, Verlag Walter de Gruyter & Co.
- KUMAR, S., STECHER, G. & TAMURA, K. (2016). MEGA7: Molecular Evolutionary Genetics Analysis Version 7.0 for Bigger Datasets. *Molecular Biology and Evolution*, **33**, 1870–1874.
- LEACHÉ, A. D., ZHU, T., RANNALA, B. & YANG, Z. (2019). The spectre of too many species. *Systematic Biology*, **68**, 168–181.
- LIBRADO, P. & ROZAS, J. (2009). DnaSP v5: a software for comprehensive analysis of DNA polymorphism data. *Bioinformatics*, **25**, 1451–1452.
- LOSOS, J. B. (2009). *Lizards in an Evolutionary Tree* (Vol. 10). Berkeley, University of California Press.
- MACEY, J. R., LARSON, A., ANANJEVA, N. B., FANG, Z. & PAPPENFUSS, T. J. (1997). Two novel gene orders and the role of light-strand replication in rearrangement of the vertebrate mitochondrial genome. *Molecular Biology and Evolution*, **14**, 91–104.
- MACEY, J. R., SCHULTE, J. A., LARSON, A., ANANJEVA, N. B., WANG, Y., PETHIYAGODA, R., RASTEGAR-POUYANI, N. & PAPPENFUSS, T. J. (2000). Evaluating trans-Tethys migration: An example using acrodont lizard phylogenetics. *Systematic Biology*, **49**, 233–256.
- MERTENS, R. (1933). Die Reptilien der Madagaskar-Expedition Prof. Dr. H. Bluntschli's. *Senckenbergiana biologica*, **15**, 260–274.
- MERTENS, R. (1966). Chamaeleonidae. *Das Tierreich*, **83**, 1–37.
- MIRALLES, A., VASCONCELOS, R., PERERA, A., HARRIS, D. J. & CARRANZA, S. (2011). An integrative taxonomic revision of the Cape Verdean skinks (Squamata, Scincidae). *Zoologica Scripta*, **40**, 16–44.
- MOCQUARD, M. F. (1900a). Diagnoses d'espèces nouvelles de reptiles de Madagascar. *Bulletin du Muséum national d'histoire naturelle*, **6**, 344–345.
- MOCQUARD, M. F. (1900b). Nouvelle contribution à la faune herpétologique de Madagascar. *Bulletin de la Société philomathique de Paris*, **9**, 93–111.
- PARCHER, S. R. (1974). Observations on the natural histories of six Malagasy Chamaeleontidae. *Zeitschrift für Tierpsychologie*, **34**, 500–523.
- PRÖTZEL, D., LAMBERT, S., ANDRIANASOLO, G., HUTTER, C., COBB, K., SCHERZ, M. & GLAW, F. (2018a). The smallest 'true chameleon' from Madagascar: A new, distinctly colored species of the *Calumma boettgeri* complex (Squamata: Chamaeleonidae). *Zoosystematics and Evolution*, **94**, 409–423.
- PRÖTZEL, D., RUTHENSTEINER, B. & GLAW, F. (2016). No longer single! Description of female *Calumma vatosoa* (Squamata, Chamaeleonidae) including a review of the species and its systematic position. *Zoosystematics and Evolution*, **92**, 13–21.
- PRÖTZEL, D., RUTHENSTEINER, B., SCHERZ, M. D. & GLAW, F. (2015). Systematic revision of the Malagasy chameleons *Calumma boettgeri* and *C. linotum* (Squamata: Chamaeleonidae). *Zootaxa*, **4048**, 211–231.

- PRÖTZEL, D., VENCES, M., HAWLITSCHKE, O., SCHERZ, M. D., RATSOAVINA, F. M. & GLAW, F. (2018b). Endangered beauties: Micro-CT cranial osteology, molecular genetics and external morphology reveal three new species of chameleons in the *Calumma boettgeri* complex (Squamata: Chamaeleonidae). *Zoological Journal of the Linnean Society*, **184**, 471–498.
- PRÖTZEL, D., VENCES, M., SCHERZ, M. D., VIEITES, D. R. & GLAW, F. (2017). Splitting and lumping: An integrative taxonomic assessment of Malagasy chameleons in the *Calumma guibei* complex results in the new species *C. gehringi* sp. nov. *Vertebrate Zoology*, **67**, 231–249.
- R CORE TEAM (2014). *R: A language and environment for statistical computing*. R Foundation for Statistical Computing, Vienna, Austria. <http://www.R-project.org/>.
- RAXWORTHY, C. J. & NUSSBAUM, R. A. (2006). Six new species of occipital-lobed *Calumma* chameleons (Squamata: Chamaeleonidae) from montane regions of Madagascar, with a new description and revision of *Calumma brevicorne*. *Copeia*, **2006**, 711–734.
- RIEPPPEL, O. & CRUMLY, C. (1997). Paedomorphosis and skull structure in Malagasy chameleons (Reptilia: Chamaeleoninae). *Journal of Zoology*, **243**, 351–380.
- SALZBURGER, W., EWING, G. B. & VON HAESSELER, A. (2011). The performance of phylogenetic algorithms in estimating haplotype genealogies with migration. *Molecular Ecology*, **20**, 1952–1963.
- SCHERZ, M. D., GLAW, F., HUTTER, C. R., BLETZ, M. C., RAKOTOARISON, A., KÖHLER, J. & VENCES, M. (2019b). Species complexes and the importance of Data Deficient classification in Red List assessments: the case of *Hylobatrachus* frogs. *PLoS One*, **14**, e0219437.
- SCHERZ, M. D., GLAW, F., RAKOTOARISON, A., WAGLER, M. & VENCES, M. (2018). Polymorphism and synonymy of *Brookesia antakarana* and *B. ambrensis*, leaf chameleons from Montagne d’Ambre in north Madagascar. *Salamandra*, **54**, 259–268.
- SCHERZ, M. D., HAWLITSCHKE, O., ANDREONE, F., RAKOTOARISON, A., VENCES, M. & GLAW, F. (2017). A review of the taxonomy and osteology of the *Rhombophryne serratopalpebrosa* species group (Anura: Microhylidae) from Madagascar, with comments on the value of volume rendering of micro-CT data to taxonomists. *Zootaxa*, **4273**, 301–340.
- SCHERZ, M. D., KÖHLER, J., RAKOTOARISON, A., GLAW, F. & VENCES, M. (2019a). A new dwarf chameleon, genus *Brookesia*, from the Marojejy massif in northern Madagascar. *Zoosystematics and Evolution*, **95**, 95–106.
- SENTÍS, M., CHANG, Y., SCHERZ, M. D., PRÖTZEL, D. & GLAW, F. (2018). Rising from the ashes: Resurrection of the Malagasy chameleons *Furcifer monoceras* and *F. voeltzkowi* (Squamata: Chamaeleonidae), based on micro-CT scans and external morphology. *Zootaxa*, **4483**, 549–566.
- STEPHENS, M., SMITH, N. J. & DONNELLY, P. (2001). A new statistical method for haplotype reconstruction from population data. *The American Journal of Human Genetics*, **68**, 978–989.
- THORPE, R., LEADBEATER, D. & POOK, C. (2005). Molecular clocks and geological dates: Cytochrome b of *Anolis extremus* substantially contradicts dating of Barbados emergence. *Molecular Ecology*, **14**, 2087–2096.
- THORPE, R., SURGET-GROBA, Y. & JOHANSSON, H. (2008). The relative importance of ecology and geographic isolation for speciation in anoles. *Philosophical Transactions of the Royal Society B: Biological Sciences*, **363**, 3071–3081.
- TILBURY, C. & TOLLEY, K. A. (2009). A new species of dwarf chameleon (Sauria: Chamaeleonidae, *Bradypodion* Fitzinger) from KwaZulu Natal South Africa with notes on recent climatic shifts and their influence on speciation in the genus. *Zootaxa*, **2226**, 43–57.
- TOLLEY, K., TOWNSEND, T. M. & VENCES, M. (2013). Large-scale phylogeny of chameleons suggests African origins and Eocene diversification. *Proceedings of the Royal Society of London B: Biological Sciences*, **280**, 11–21.
- VASCONCELOS, R., PERERA, A., GENIEZ, P., HARRIS, D. J. & CARRANZA, S. (2012). An integrative taxonomic revision of the *Tarentola* geckos (Squamata, Phyllodactylidae) of the Cape Verde Islands. *Zoological Journal of the Linnean Society*, **164**, 328–360.
- VLETTE, P. (1991). Principales localités où des insectes ont été recueillis à Madagascar: Chief field stations where insects were collected in Madagascar. *Faune de Madagascar, Supplement*, **2**, 1–88.
- WICKHAM, H. (2016). *ggplot2: Elegant Graphics for Data Analysis*. New York (USA), Springer-Verlag.

Zoobank Registrations

at <http://zoobank.org>

This published work and the nomenclatural acts it contains have been registered in ZooBank, the online registration system for the International Commission on Zoological Nomenclature (ICZN). The ZooBank LSIDs (Life Science Identifiers) can be resolved and the associated information can be viewed through any standard web browser by appending the LSID to the prefix <http://zoobank.org>. The LSID for this publication is as follows:

urn:lsid:zoobank.org:pub:2108AD7F-C228-4926-B108-CFE-9BAE94BBF

Electronic Supplement File

at <http://www.senckenberg.de/vertebrate-zoology>

File 1: Suppl_Table_1_Morphological_measurements_of_*C_nasutum*_group_specimens.xlsx. — DOI: 10.26049/VZ70-1-2020-03/1